



Arab American University

Faculty of Graduate Studies

The effect of Rashba spin-orbit interaction and magnetic field on the thermo-magnetic properties of an electron confined in a 2D semiconductor quantum dot

By

Nouf Ibrahim Zaki Ibrahim

Supervisor

Dr. Muayad Abu Saa'

Co-Supervisor

Prof. Mohammad ElSaid

This Thesis was submitted in partial fulfillment of the requirements for the Master's degree in Physics

January/2020

©Arab American University-2020. All rights reserved.

Thesis Approval

**The effect of Rashba spin-orbit interaction and magnetic field on the
thermo-magnetic properties of an electron confined in a 2D semiconductor
quantum dot**


By


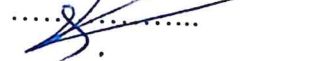
Nouf Ibrahim Zaki Ibrahim

This thesis was defended successfully on 11th.Jan.2020 and approved by:

Committee members:

1. Assist. Prof. Dr. Muayad Abu Saa' (Supervisor)
2. Prof. Dr. Mohammad ElSaid (Co-Supervisor)
3. Assoc. Prof. Dr. Ahmad Omar (Internal Examiner)
4. Assist. Prof. Dr. Mustafa Abu Safa (External Examiner)

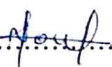
Signature

.....

.....

.....

.....

Declaration

I am Nouf Ibrahim Zaki Ibrahim , student of Faculty of Graduate Studies of the Arab American University – Palestine , declare and certify with my signature that my thesis entitled **The effect of Rashba spin-orbit interaction and magnetic field on the thermomagnetic properties of an electron confined in a 2D semiconductor quantum dot** is entirely the result of **my own work** and does not contain material previously published, except where this appropriately cited through full and accurate referencing.

Student's Name: Nouf Ibrahim Zaki Ibrahim

Signature: .....

Date: 16.7.2020

Dedication

I dedicate this great achievement to the woman who taught me and brought me up and was my first support after God,

To my beloved and dear mother, may God protect you.

To the distant soul of my dear father, who always accompanies me -may God have mercy on him -.

To my heart's twin and my partner, my dear sister,

To those who helped and supported me in my life and scientific career, to my dear brothers, Zaki, Mohammad and Abdul Rahman, may God protect you.

To all my friends, colleagues and to those who were beside me and I was pleased to know him.

To everyone who spared no effort in helping me, and who did not skimp on teaching me even a letter and were aiding me in the path to success.

Acknowledgments

Initially, many great praises and thanks to God for successfully completing this thesis.

I would like to extend my thanks and appreciation to my supervisor, Dr. Muayad Abu Saa`, who helped me in choosing my distinguished future path and assisted me in my academic studies.

And to my supervisor, Professor Mohamed El-Said, for his great and valuable efforts, his follow-up and advice to me during the work phase of this scientific research.

I would like to thank all the scientific research team, Mr. Ayham AlShaer, for his assistance in the mathematica program and in many things, and Mr. Mahmoud Ali for his support and help to me.

Abstract

The energy spectra of Hamiltonian of a single electron confined in a parabolic quantum dot, in the presence of Rashba spin orbit interaction term effect, applied uniform magnetic field and topological defect had been reproduced in a closed form. The quantum dot energy spectra are used to compute the statistical mean energy and from which we obtain the thermodynamic and magnetic quantities, namely: heat capacity, magnetization and magnetic susceptibility. We show their dependences on the Hamiltonian physical parameters. The magnetic phase diagrams of the quantum dot material are shown as function of temperature, Rashba parameter and magnetic field.

The results reveal that the magnetic field, temperature, confining frequency, in addition to Rashba and topological effects significantly affect the thermo-magnetic properties of the Quantum dot.

The computed results show that quantum dot material changes its magnetic type from diamagnetic to paramagnetic as demonstrated in the magnetic phase diagrams contour plots. Furthermore, the behavior of the heat capacity of the QD is shown as a function of QD-Hamiltonian physical parameters.

Our computed results are tested against the corresponding theoretical reported ones.

Table of contents:

No.	Title	Page No.
Thesis Approval		ii
Dedication		iv
Acknowledgments		vi
Abstract		Vii
Table of contents		ix
List of Tables		xi
List of Figures		xii
List of Symbols and Abbreviations		xv
Chapter one	Introduction	1
	1.1 Nanomaterials.	1
	1.2 Applications of quantum dot.	4
	1.3 Rashba effect.	7
	1.4 Literature Review.	8
	1.5 Research objectives.	9
Chapter Two	Theory of Quantum Dot Hamiltonian.	10
	2.1 The Hamiltonian theory of a single electron quantum dot.	10
	2.2 Topological Effect.	12
	2.3 Energy spectra expression and statistical average energy.	13
	2.4 The magnetic and thermal quantities for GaAs QDs.	15
	2.4.1 The magnetization and magnetic susceptibility.	15

	2.4.2 The Heat capacity.	16
Chapter Three	Results and discussions.	17
	3.1 QD spectra and statistical energy.	18
	3.2 Magnetic properties: Magnetization (M) and susceptibility (χ).	31
	3.3 Thermal properties: Heat capacity (C_v).	39
	3.4 Magnetic phase transition.	43
Chapter Four	Conclusion and Future work.	49
References		51
المخلص		60

List of Tables:

No.	Title	Page No.
Table (3.1)	labeled the Fock-Darwin energy states.	18

List of Figures:

No.	Title	Page No.
Figure 1.1	DOS vs. Energy for bulk material, quantum well, quantum wire and quantum dot.	2
Figure 1.2	Rashba Spin Orbit interaction in Spintronics.	5
Figure 1.3	Schematic representation of GaAs/AlGaAs.	6
Figure 2.1	Topological defect described in polar coordinates.	12
Figure 3.1	The Fock-Darwin energy spectrum at $\omega_0 = 2.5 R^*$, $p = 1$ and $\gamma = 0 a^*. R^*$.	19
Figure 3.2	The energy for $n=0$ vs ω_c with $\gamma=0$ and $0.7 a^*. R^*$, when $p=1$, $\omega_0=2.5 R^*$ at a) $l=-1$, b) $l=0$ and c) $l=1$.	21
Figure 3.3	The energy for $n=0$ vs ω_c with $p=1$ and 1.5 , when $\gamma=0 a^*. R^*$, $\omega_0=2.5 R^*$ at a) $l=1$, b) $l=0$ and c) $l=1$.	24
Figure 3.4	The $\langle E \rangle$ vs # of basis with different T at $\omega_c=3R^*$, $\omega_0=2.5R^*$, $\gamma = 0.5 a^*. R^*$ and $p=1$.	25
Figure 3.5	$\langle E \rangle$ vs ω_c with $\omega_0=2.5 R^*$ and $T=5K$.	27
Figure 3.6	$\langle E \rangle$ vs T with $\omega_c=3R^*$, $\omega_0=2.5 R^*$ and in state a) $p=1$ and b) $p=1.5$.	28
Figure 3.7	$\langle E \rangle$ vs T with $\omega_c=3R^*$, $\omega_0=2.5 R^*$ and in state a) $\gamma=0 a^*. R^*$, and b) $\gamma=0.7 a^*. R^*$.	30
Figure 3.8	M vs ω_c with $\omega_0=2.5 R^*$ and $T=5K$.	31
Figure 3.9	M vs T with $\omega_c=3R^*$, $\omega_0=2.5 R^*$ and in state a) $p=1$ and b) $p=1.5$.	33
Figure 3.10	M vs T with $\omega_c=3R^*$, $\omega_0=2.5 R^*$ and in state a) $\gamma=0 a^*. R^*$ and b) $\gamma=0.7 a^*. R^*$.	34
Figure 3.11	χ vs ω_c with $\omega_0=2.5 R^*$ and $T=5K$.	35

Figure 3.12	χ vs T with $\omega_c = 3R^*$, $\omega_0 = 2.5 R^*$ and in state a) $p=1$ and b) $p=1.5$.	37
Figure 3.13	χ vs T with $\omega_c = 3R^*$, $\omega_0 = 2.5 R^*$ and in state a) $\gamma = 0 a^*.R^*$ and b) $\gamma = 0.7 a^*.R^*$	38
Figure 3.14	C_v vs ω_c with $\omega_0 = 2.5 R^*$ and $T=5K$.	39
Figure 3.15	C_v vs T with $\omega_c = 3R^*$, $\omega_0 = 2.5 R^*$ and in state a) $p=1$ and b) $p=1$.	40
Figure 3.16	C_v vs T with $\omega_c = 3R^*$, $\omega_0 = 2.5 R^*$ and in state a) $\gamma = 0 a^*.R^*$ but b) $\gamma = 0.7 a^*.R^*$.	42
Figure 3.17	Magnetic phase diagram of GaAs QD as a function of the temperature and magnetic field with $\omega_0 = 6.3R^*$, $p=1$ and $\gamma = 0 a^*.R^*$.	43
Figure 3.18	Magnetic phase diagram of GaAs QD as a function of the T and ω_c with $\omega_0 = 0.5R^*$ for a) $p=1$, $\gamma = 0 a^*.R^*$, b) $p=1$, $\gamma = 0.35 a^*.R^*$, c) $p=1.2$, $\gamma = 0 a^*.R^*$ and d) $p=1.2$ and $\gamma=0.35 a^*.R^*$. The golden region corresponds to the paramagnetic phase ($\chi > 0$) whereas the blue region to the diamagnetic phase ($\chi < 0$).	46
Figure 3.19	Magnetic phase diagram of GaAs QD as a function of the ω_c and γ with $\omega_0 = 0.5R^*$ and $p=1$ for a) $T=20 K$, b) $T=250K$. The golden region corresponds to the	47

	paramagnetic phase ($\chi > 0$) whereas the blue region to the diamagnetic phase ($\chi < 0$).	
Figure 3.20	Magnetic phase diagram of GaAs QD as a function of the ω_c and p with $\omega_0 = 0.5R^*$ and $\gamma = 0$ $a^*.R^*$ for $a)$ $T = 20$ K, $b)$ $T = 250$ K. The golden region corresponds to the paramagnetic phase ($\chi > 0$) whereas the blue region to the diamagnetic phase ($\chi < 0$).	48

List of Symbols and Abbreviations:

QD	Quantum Dot
QW	Quantum Well
QWW	Quantum Well Wire
GaAs	Gallium Arsenide
AlGaAs	Aluminum Gallium Arsenide
RSOI	Rashba Spin-Orbit Interaction
DOS	Density Of States
3D	Three Dimensions
2D	Two Dimensions
1D	One Dimension
0D	Zero Dimension
E_n	Energy spectrum
$\langle E \rangle$	Statistical average energy
M	Magnetization
χ	Magnetic Susceptibility
C_v	Heat Capacity
γ	RSOI coupling factor

p	Topological factor
α	Kink parameter
Ω	Effective frequency
ω_c	Cyclotron frequency
ω_0	Confining frequency
B	Magnetic field flux
e	free electron charge
m_0	free electron mass
m^*	Effective mass of electron
meV	millielectron volt
P	Linear momentum
A	Vector potential
c	Speed of light
T	Temperature
K	Kelvin degree
nm	nano meter
k_B	Boltzmann constant
n	Radial quantum number
R^*	Effective Rydberg energy unit
a^*	Effective Bohr radius

\hbar	Reduced Planck's constant
\uparrow	Electron's spin in up direction
\downarrow	Electron's spin in down direction

Chapter one

Introduction

Technological developments are continually progressing to become smaller, faster and more accurate. So, nanoscience has become a rich science of research to study the different properties and features of various types of materials in this scale.

1.1 Nanomaterials:

Nano-technology is observed in materials and structures having dimensions in the billionth of a meter (in the range of 10 to 200 Angstroms).

Nanomaterial's are classified into four types according to the number of dimensions that electron can move freely without confinement in the material [1]:

1. Bulk material: An electron moves freely in all dimensions (3D).
2. Quantum well material (QW): Electrons move freely in two dimensions but are confined in the third dimension.
3. Quantum Well Wire material (QWW): Electrons can move inside the material freely in one dimension, while motion is quantized in the other 2-dimensions.
4. Quantum dot material (QD): The electron cannot move freely and is confined in all three dimensions [2-3].

Because we can control the direction of the electron's movement, this affects greatly energy spectra and density of state (DOS) as shown in Figure (1.1):

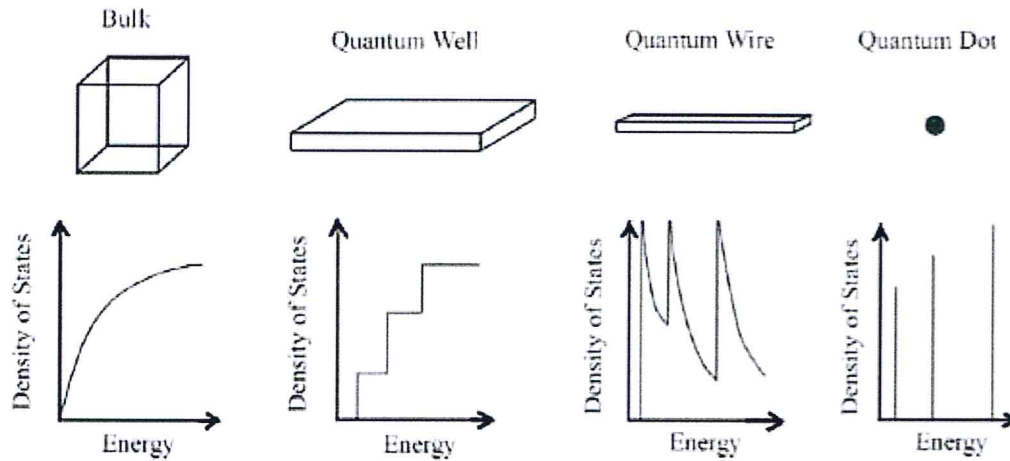


Figure (1.1): DOS vs. Energy for bulk material, quantum well, quantum wire and quantum dot [4].

QDs or artificial atoms are nanoscale systems that can contain few electrons, and its length scale varies from 2 to 10 nanometers [5-6].

The shape and size of the QD can be also experimentally tuned over a wide range leading to a system with controllable physical properties. Heterostructure QDs fabricated as two or more semiconductor layers with negative voltage applied to the metal electrodes leading to carrier's confinement in all three spatial dimensions [7-9].

The developments in nanofabrication methods make the confinement of the finite number of electrons in a localized three-dimensional space in a nano-dimension also possible [10].

1.2 Applications of QD:

Semiconductor nanostructures QDs have become very hot research subject due to their potential device applications such as: QD laser, quantum computation, QD solar cell, biological, and medical application like the image cancer treatment [11-13].

The spin-orbit coupling effect in semiconductor QD system is very important as it plays an essential role in controlling the properties of the QD which makes the QD excellent basis in the new growing field of device technology, called spintronics. The QD-spin transistor is considered to be an important electronic device in the area of spintronics.

The spin orbit interaction (SOI) term is, particularly, very interesting because it controls direction of the carriers in nanomaterials which form new type of devices called spintronics. The SOI coupling, which arises due to structural inversion symmetry in nanostructures, is defined as the interaction between the spin of a confined electron in the nanomaterial and the magnetic field induced by the heterostructure local electric field due to the potential variation at the interface of GaAs/AlGaAs material.

The strength of this term can be manipulated experimentally by an external gate voltage or equivalently an applied external electric field through the contact gate with the heterostructure materials as shown in Figure (1.2) [14].

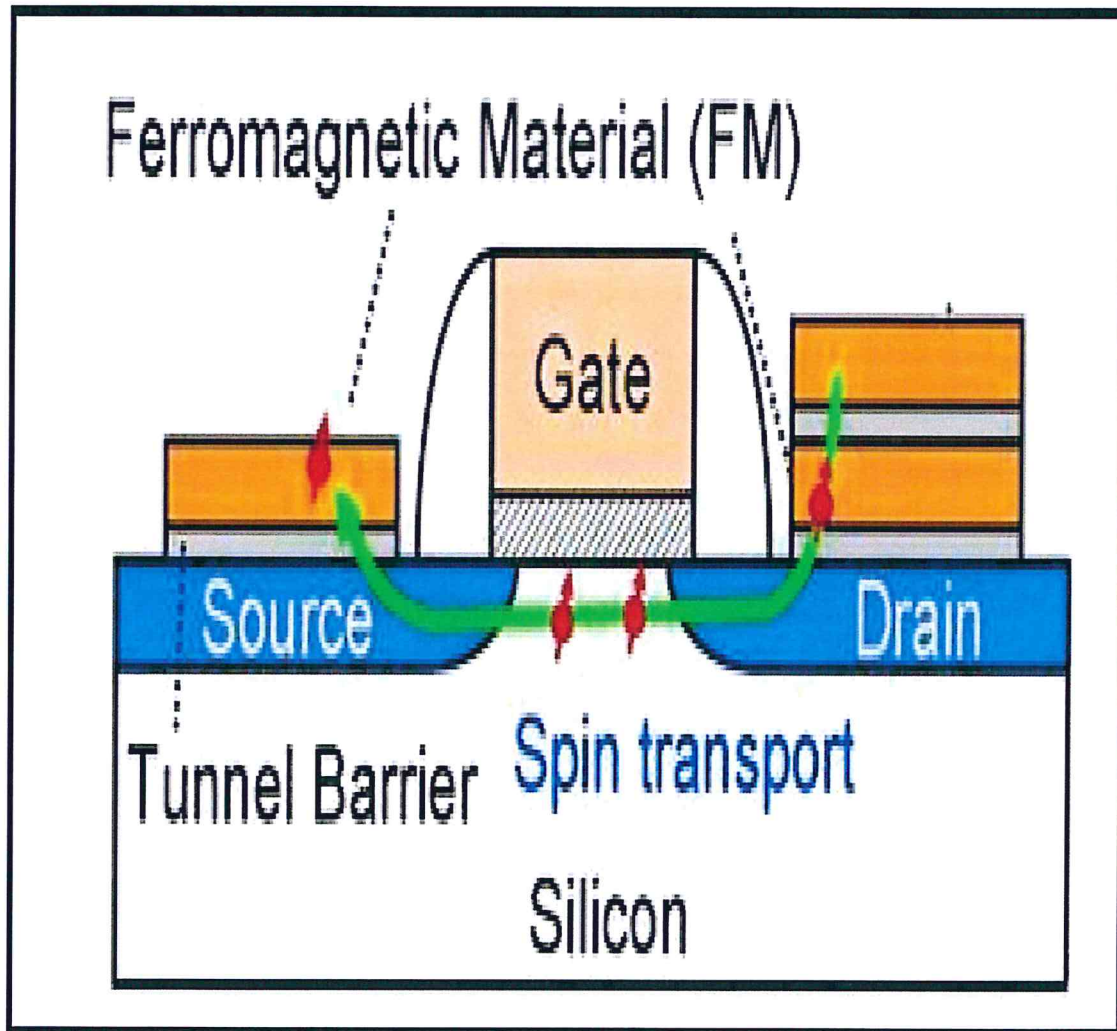


Figure (1.2): Rashba Spin Orbit interaction in Spintronics devices [14].

Single and double quantum dots fabricated from GaAs/AlGaAs heterostructure material are shown schematically in Figure (1.3a, b and c).

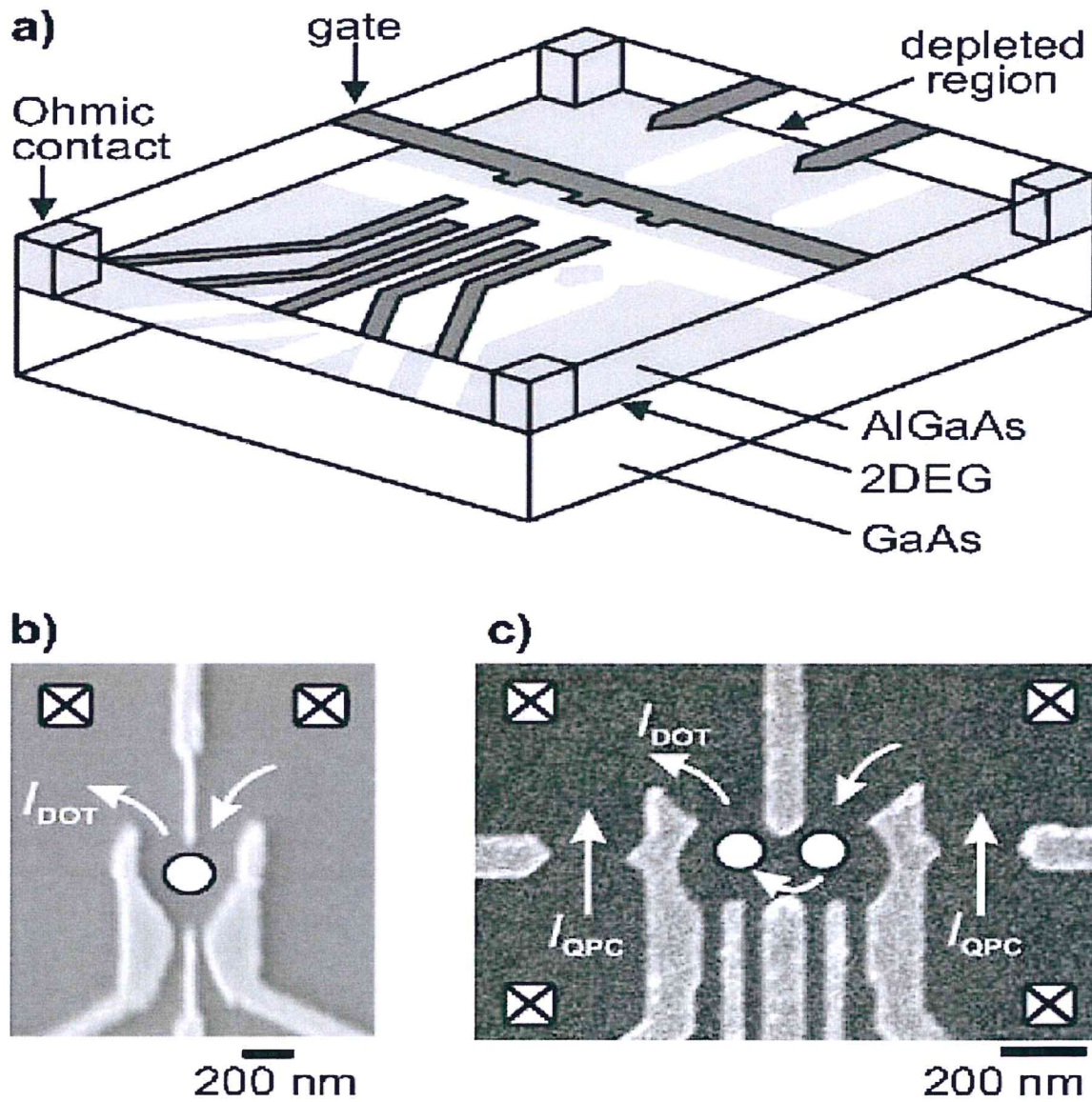


Figure 1.3(a, b and c): Schematic representation of GaAs/AlGaAs quantum dots [15].

1.3 Rashba effect:

The addition of a magnetic field and Rashba term makes the QD_Hamiltonian function very interesting research problem in the field of nanoscience and nanotechnology.

The strength of this Rashba term can be manipulated experimentally by an external gate voltage or equivalently an applied external electric field through the contact gate with the heterostructure materials. The phenomena of Rashba effect helps us to control the electron spin direction and thus to design the QD as a non-magnetic source/drain spintronic device.

The ferromagnetic source and ferromagnetic drain are necessary requirements for functioning the Datta-Das transistor. The production of this device is still challenging due to the problems with efficient spin injection from ferromagnetic source and drain. The Rashba SOI, plays an important role and gives us new operational principle for designing the QD as a transistor.

1.4 Literature Review:

Different authors had, recently, studied the thermodynamic and magnetic properties of QD systems in the presence of a magnetic field [16-17]. The combined effects of pressure, topological factor and the spin-orbit interaction on the QD energy spectra had also been considered [18-19]. Chatterjee et al, studied the magnetization and susceptibility for two electrons in a QD in the presence of electron-electron interaction and SOI [20]. Avetisyan et al. investigated the interaction between three and four electrons under effect of magnetic field and spin orbit interaction [21].

Xun Wang et.al. had presented the effect of quantum confinement on the electronic properties of the QD and QWW nano structure materials [22].

Elsaid et al had used exact diagonalization, variational and $1/N$ expansion methods to investigate the thermodynamic, electronic and magnetic properties of a single and coupled QDs [23-31]. Chatterjee and Boyacioglu studied the susceptibility of QD with Gaussian confinement [32], while Tapash and Pietilainen considered an electron confined in QD with Rashba coupling effect [33].

1.5 Research objectives:

In this thesis, we will study in details the effect of spin-orbit interaction term on properties of the QD. We consider a single electron QD confined in two dimensions in the presence of a magnetic field, in addition to the spin-orbit interaction term, to reproduce the complete attainable energy spectra of the corresponding solvable QD-Hamiltonian system. The obtained energies will enable us to investigate the variation of energy levels, magnetic and thermal properties of the zero-dimensional semiconductor QD systems with the Rashba term.

There are two main aims of this research that can be summarized as follows:

1. To reproduce the eigenenergy spectra of the solvable QD Hamiltonian with both magnetic field and Rashba spin orbit interaction term and obtain the energy spectra expression in terms of the QD parameters.
2. To calculate the thermal and magnetic properties of the QD and show their behaviors as functions of the Rashba term parameter.

Chapter Two

Theory of Quantum Dot Hamiltonian

2.1 The Hamiltonian theory of a single electron QD:

The Hamiltonian of an electron confined in QD by a potential , $V_c(r)$, and under the effect of an applied uniform magnetic field and spin-orbit interaction term can be given as:

$$\hat{H} = \frac{1}{2m^*} [\vec{P} + \frac{e}{c} \vec{A}]^2 + V_c(r) + H_R \quad \dots (2.1)$$

where \vec{P} refers to the electron momentum operator.

\vec{A} is the vector potential which is related to the magnetic field \vec{B} as

$$\vec{B} = \vec{\nabla} \times \vec{A} . \quad \dots (2.2)$$

The vector potential is chosen to be in the symmetric gauge as

$$A = \frac{B}{2}(-y, x, 0) \quad \dots (2.3)$$

B is assumed to be uniform and normal to the QD plane along the z - axis.

e is the elementary charge,

c is the speed of light,

Finally, $V_c(r)$ is the confining potential, modeled as a parabolic type like,

$$V_c(r) = \frac{1}{2} m^* \omega_0^2 r^2, \quad \dots (2.4)$$

where, ω_0 is the strength of the confinement potential frequency,

r is the position vector of an electron in the QD and its equal $(x^2 + y^2)^{\frac{1}{2}}$,

m^* is the electron effective mass of the material of GaAs QDs,

The spin-orbit interaction Hamiltonian can be presented as:

$$H_R = \alpha_R \vec{\sigma} \cdot [\vec{\nabla} V(r) \times (\vec{p} - \frac{e}{c} A)] / \hbar \quad \dots (2.5)$$

where: H_R is the Rashba term,

α_R is the Rashba parameter strength of SOI,

σ are the Pauli matrices, $\{\sigma_x, \sigma_y\}$,

\hbar is Plank's constant.

2.2 Topological Effect:

The surface of the quantum dot has a topological defect described as in Figure (2.1) in polar coordinates (ρ, φ) by the metric [34]:

$$dl^2 = d\rho^2 + \rho^2 d\varphi^2 \quad \dots (2.6)$$

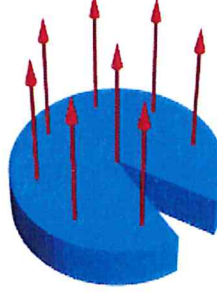


Fig. (2.1): Topological defect described in polar coordinates [34].

where, $\rho = \alpha^{-1}r$... (2.7)

$$\varphi = \alpha\theta \quad \dots (2.8)$$

then the metric becomes,

$$dl^2 = \alpha^{-2}dr^2 + r^2 d\theta^2 \quad \dots (2.9)$$

while α is a kink parameter and it control the cut off, whereas $0 < \alpha < 1$, if $\alpha = 1$ means that there is no effect of topological defect.

with φ belongs to $0 < \varphi < 2\pi\alpha$, and $0 < \theta < 2\pi$.

2.3 Statistical average energy:

The total quantum dot Hamiltonian, H , can be reduced to a solvable harmonic oscillator Hamiltonian with analytical energy spectra expression. The eigenenergy spectra is defined, in terms of the quantum numbers (n, l) and other physical parameters [34], as:

$$\begin{aligned}
E_{n,l,s}(\omega_0, \omega_c, \gamma, p) = & \hbar\Omega(2n + p|l| + 1) + \frac{p^2}{2}\hbar\omega_cl \\
& + \left(\gamma m^* \omega_0^2 l + \frac{1}{4}g^* \hbar\omega_c\right)s \quad \dots (2.10)
\end{aligned}$$

Where Ω is the effective frequency and defined as:

$$\Omega^2 = \left(1 + s\gamma \frac{m^* \omega_c}{\hbar}\right) \omega_0^2 + \left(\frac{\omega_c p}{2}\right)^2 \quad \dots (2.11)$$

$$\omega_c = \frac{eB}{m^* c} \quad \dots (2.12)$$

ω_c denotes the cyclotron frequency,

s is the spin of the electron,

γ is the Rashba spin orbit parameter,

p is the topological parameter and it equal the inverse of kink parameter (α^{-1}),

n is the radial quantum number,

l is the angular quantum number,

g^* is the effective Lande factor.

The obtained eigen energies of the QDs will be used as input essential data to calculate the statistical average energy,

$$\langle E_{n,l,s}(\omega_0, \omega_c, \gamma, p) \rangle = \frac{\sum_{\alpha=1}^i E_{\alpha} e^{-E_{\alpha}/K_{\beta} T}}{\sum_{\alpha=1}^i e^{-E_{\alpha}/K_{\beta} T}} \quad \dots (2.13)$$

The summation (α) is taken over the energy levels (n and l) of the QD. We will use the computer program to calculate this summation for different ranges of temperature and confining potential.

2.4 The magnetic and thermal quantities for GaAs QDs:

Having computed the average energy, all the thermal and magnetic quantities of the QD can be obtained, using the common statistical expression given in the statistical physics books.

2.4.1 The magnetization and magnetic susceptibility:

Magnetization is a description of how magnetic materials affected with the magnetic field, and it is the first derivative of the statistical energy of the QD [28]:

$$M = - \frac{\partial \langle E_{n,l,s}(\omega_0, \omega_c, \gamma, p) \rangle}{\partial B} \quad \dots (2.14)$$

Magnetic Susceptibility indicates whether the material is attracted to ($\chi > 0$) paramagnetic or repulsive of ($\chi < 0$) diamagnetic the magnetic field. χ can be calculated from M using the following relation [35]:

$$\chi = \frac{\partial M}{\partial B} \quad \dots (2.15)$$

2.4.2 The Heat capacity:

Heat Capacity is defined as the amount of heat that is needed to raise the material's temperature by (1°C) one degree, and it's the derivative of the average energy with respect to temperature [36]:

$$C_V = \frac{\partial \langle E_{n,l,s}(\omega_0, \omega_c, \gamma, p) \rangle}{\partial T} \quad \dots (2.16)$$

The dependence of the thermal and magnetic variables will be investigated as functions of confinement strength, magnetic field cyclotron frequency, Rashba term, topological factor and temperature. In addition, the phase diagram for the magnetic susceptibility will be plotted as function of the physical parameters to show the magnetic transition of the GaAs from diamagnetic to paramagnetic.

Chapter Three

Results and discussions

In this chapter we discuss the obtained results for the energy spectra of an electron confined in a parabolic QD in presence of RSOI term, topological effect and an applied uniform magnetic field.

We study the physical properties of the GaAs QDs material by computing the: Statistical energy, magnetization, susceptibility and heat capacity.

For GaAs QD, we used the following physical parameters:

Effective electron mass: $m^* = 0.067m_e$

Effective Lande factor: $g^* = -0.44$

Effective Rydberg energy: $R^* = 5.694 \text{ meV}$

Effective Bohr radius: $a^* = 9.8 \text{ nm}$

Rashba parameter γ ($1 \text{ a}^*. R^* = 55.8 \text{ meV.nm}$)

Magnetic field ω_c ($\omega_c(R^*) = 0.296 \times (B \text{ in Tesla } (T))$)

3.1 Quantum dot spectra and statistical energy:

In this section, we study the effect of RSOI and topological parameters on the energy states for the GaAs QD.

In Fig. (3.1), we have used equation (2.10) to plot the QD Fock-Darwin states as a function of a magnetic field strength for $p=1$, $\omega_0=2.5 R^*$ and zero Rashba parameter $\gamma=0 a^*. R^*$. The energy spectra show a similar behavior with the corresponding ones given by Ref. [37].

The following table (3.1) shows the states labels at $\omega_c=1R^*$ from the bottom:

Table (3.1): Labeled the Fock-Darwin energy states plotted in Fig. (3.1).

$ n, l, s\rangle$	$ n, l, s\rangle$
$ 0, 0, +\rangle$	$ 0, 0, -\rangle$
$ 0, -1, +\rangle$	$ 0, -1, -\rangle$
$ 0, 1, +\rangle$	$ 0, 1, -\rangle$
$ 0, -2, +\rangle$	$ 0, -2, -\rangle$
$ 1, 0, +\rangle$	$ 1, 0, -\rangle$
$ 0, 2, +\rangle$	$ 0, 2, -\rangle$
$ 1, -1, +\rangle$	$ 1, -1, -\rangle$
$ 1, 1, +\rangle$	$ 1, 1, -\rangle$
$ 1, -2, +\rangle$	$ 1, -2, -\rangle$
$ 1, 2, +\rangle$	$ 1, 2, -\rangle$

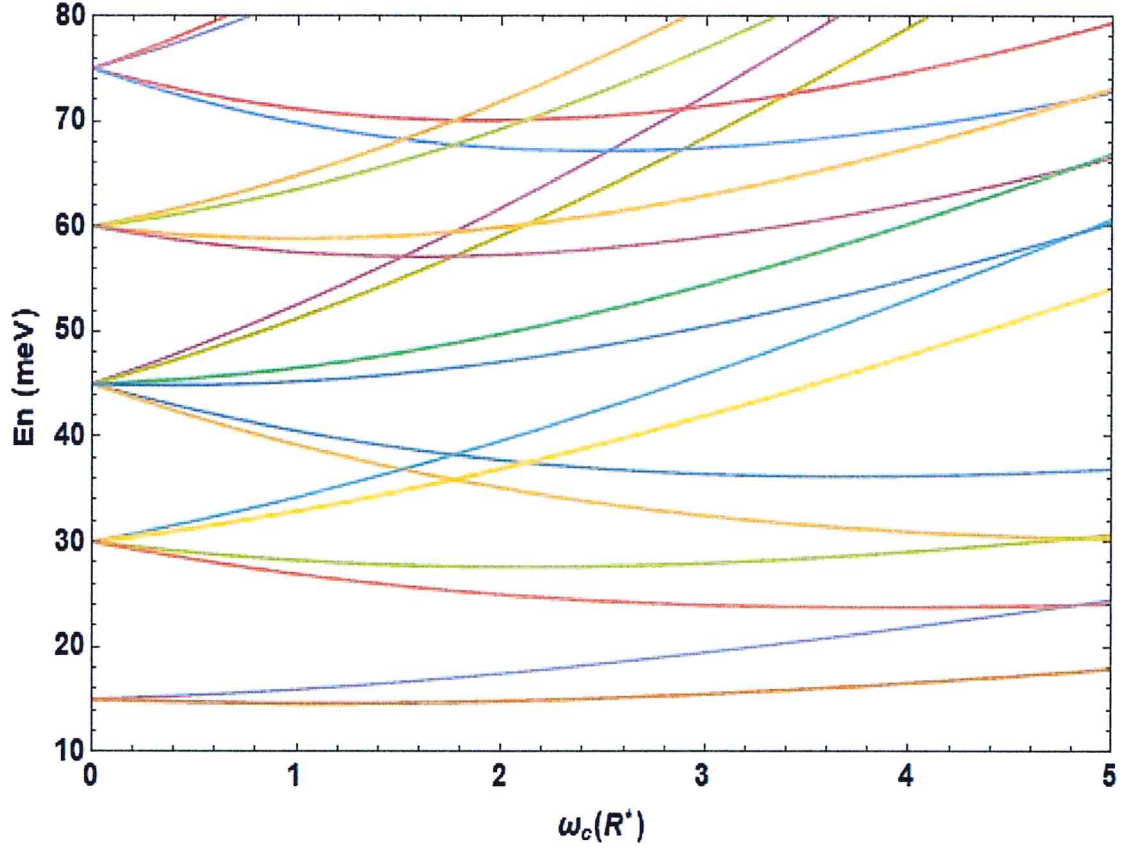


Fig (3.1): The Fock-Darwin energy spectrum at $\omega_0 = 2.5 R^*$, $p = 1$ and $\gamma = 0 a^* R^*$.

Fig. (3.2) shows the energy spectra as function of the magnetic field strength ω_c in presence of RSOI effect on the ground state ($n=0$) for $l=-1$ (Fig. 3.2a), $l=0$ (Fig3.2b) and $l=1$ (Fig 3.2c) and topological parameter $p=1$.

for $l=0$ and 1, energy values for the spin up (\uparrow) with γ effect, increases at fixed ω_c , but in spin down (\downarrow) it decreases. However; for state with negative angular momentum $l=-1$, the energy values behave in opposite manner for $\omega_c \leq 3.8 R^*$.

This energy behavior is clear from energy expression given by equation (2.10), because the second term ($\frac{p^2}{2} \hbar \omega_c l$) includes l which controls the sign more than other terms.

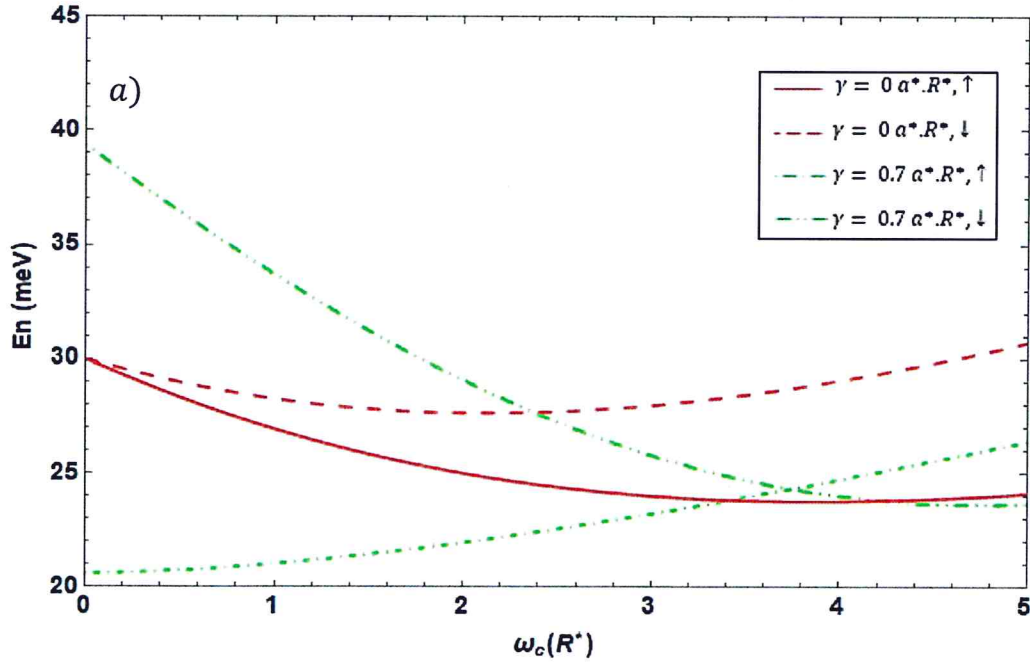


Fig. (3.2): The energy for $n=0$ vs ω_c with $p=1$, $\omega_0=2.5 R^*$ at a) $l=-1$, b) $l=0$ and c) $l=1$.

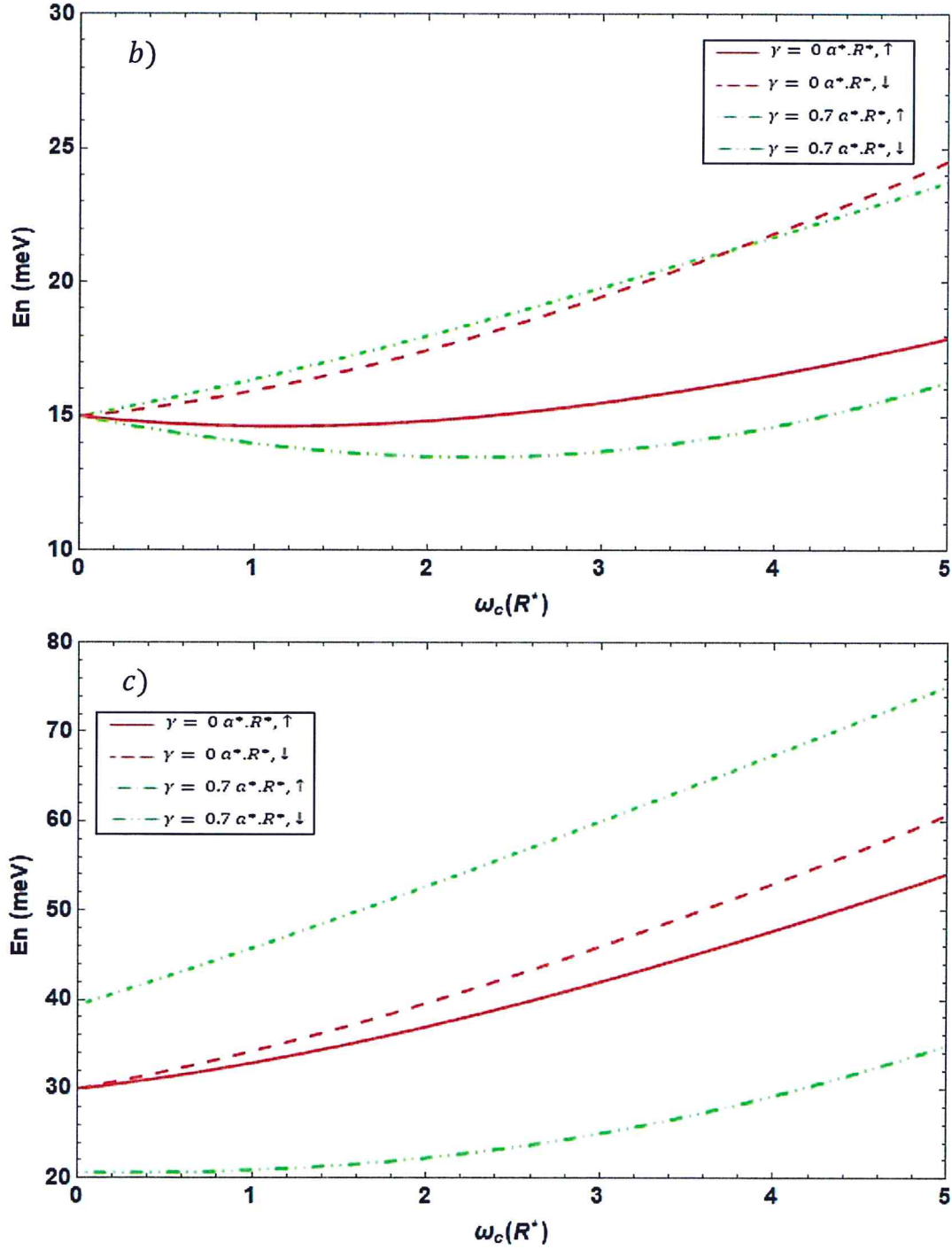


Fig. (3.2): The energy for $n=0$ vs ω_c with $p=1$, $\omega_0=2.5 R^*$ at *a*) $l=-1$, *b*) $l=0$ and *c*) $l=1$.

The behavior of the energy spectra is mainly due to the effect of RSOI, $p=1$. The term affects directly the effective frequency (Ω) and spin Zeeman terms in equation (2.10).

In this case, the RSOI lowers the effective frequency for the spin down (\downarrow) and increases the frequency for spin up (\uparrow). In addition, it increases or decreases the energy for positive l ($+l$) and negative l ($-l$), respectively.

These two factors modify the energy of the electron confined in a quantum dot

So, the amount of energy for the confined electron is decreased and energy are splitting to sub level in presence of the magnetic field.

The opposite results are observed for $l = -1$ because of the negative sign (-), which comes from the angular quantum number in equation (2.10). These results are in agreement with Bychkov in Ref. [33].

However, when studying the effect of topological defect (p) we observe that energy state increases at constant ω_c for spin up and down as shown in Figures [(3.3a at $l=-1$, 3.3b at $l=0$ and 3.3c at $l=1$)] with $\gamma = 0$ $a^*.R^*$.

For $l=0$ and 1 , the energy level increases as ω_c increases, while the energy decreases for the case of $l=-1$ at $\omega_c = 3R^*$ and then increases, because of confining the electron in a small region which leads to an enhancement in the momentum by uncertainty principle [38] and eventually the energy of the electron increases.

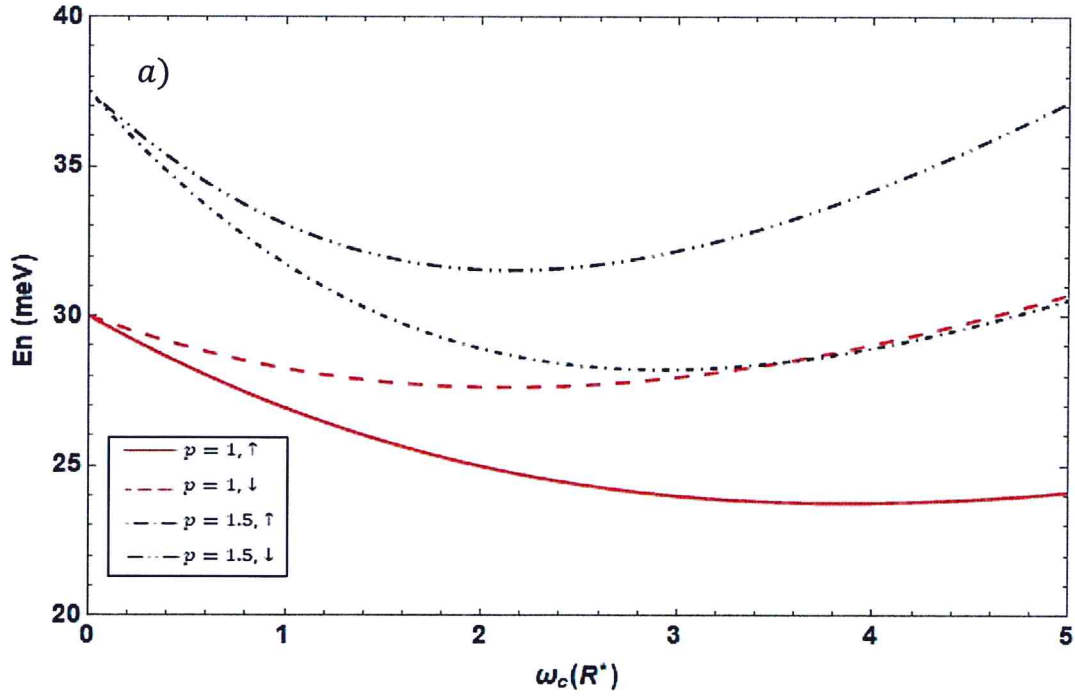


Fig. (3.3): The energy for $n=0$ vs ω_c with $\gamma = 0$ $a^*.R^*$, $\omega_0 = 2.5 R^*$ at a) $l=-1$, b) $l=0$ and c) $l=1$.

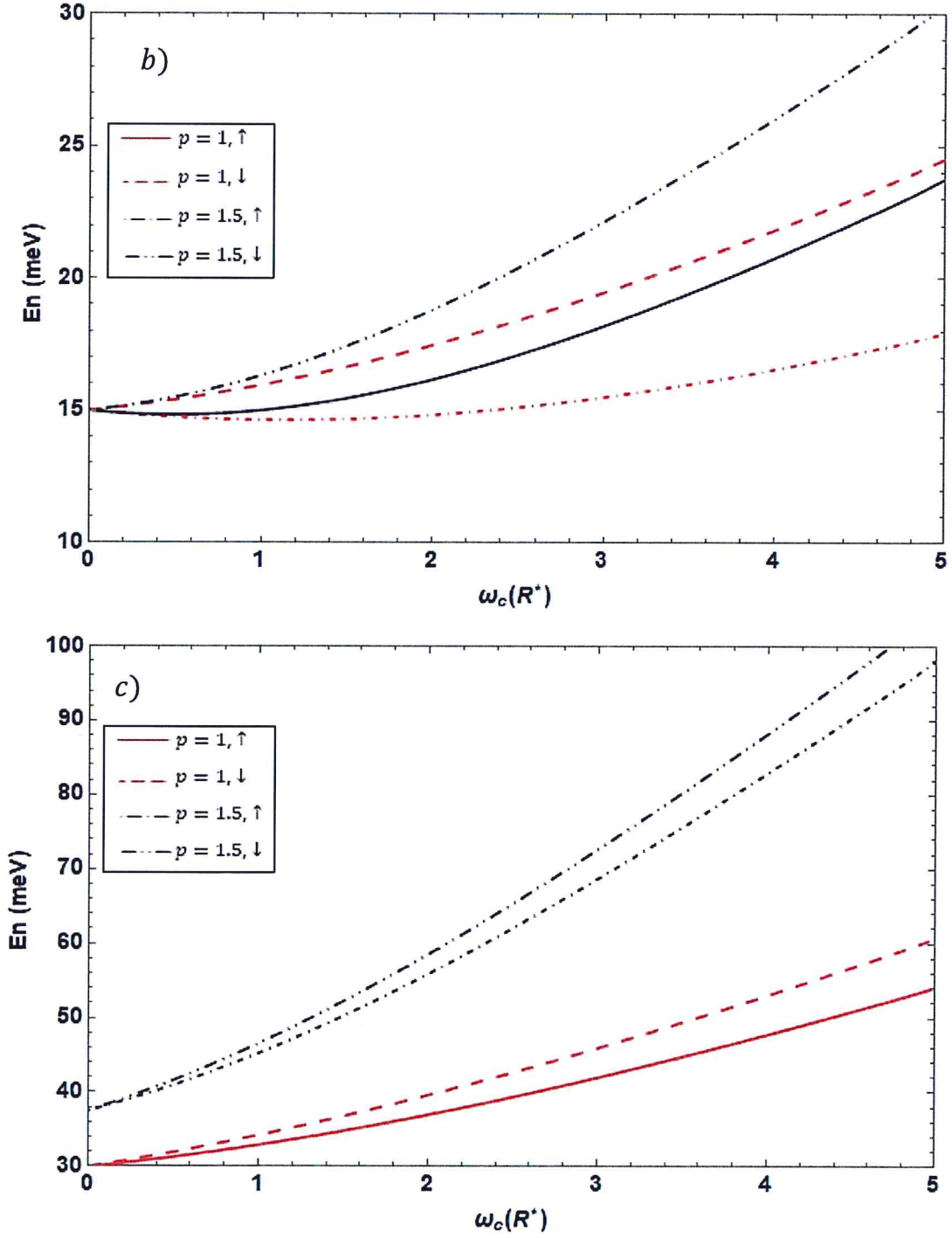


Fig. (3.3): The energy for $n=0$ vs ω_c with $\gamma = 0$ $a^*.R^*$, $\omega_0 = 2.5 R^*$ at a) $l=-1$, b) $l=0$ and c) $l=1$.

The first and important step in our work is to ensure convergency of the average statistical energy of the QD. We plot the statistical energy using equation (2.10) as function of number of basis for various temperature $T=10\text{K}$, $T=30\text{K}$ and $T=100\text{K}$.

Fig. (3.4) shows the average energy $\langle E \rangle$ calculated by taking quite large number of basis: l ($-7 \rightarrow 7$) and n ($0 \rightarrow 5$). For low temperature range ($T=10$ and 30 K), a small number of basis is needed, however, a large number of basis is needed ($\sim \#60$) for temperature $T=100\text{ K}$. The number of choices $\#60$ is good choices, as indicate by the vertical line shown in the Figure.

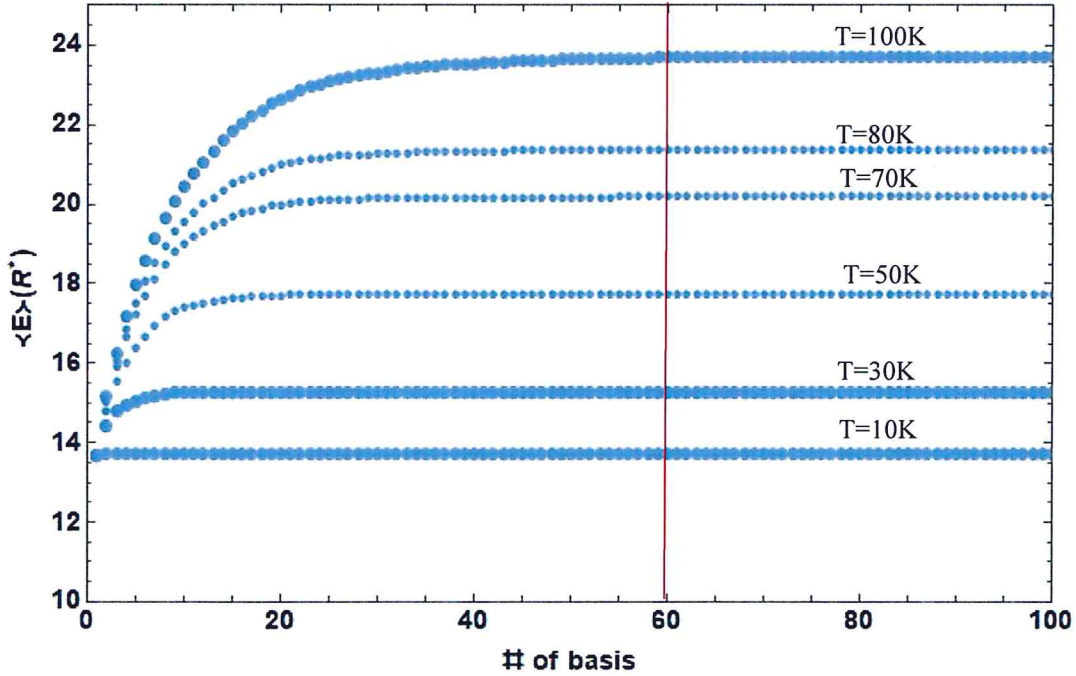


Fig. (3.4): The $\langle E \rangle$ vs # of basis with different T at $\omega_c = 3R^*$, $\omega_0 = 2.5 R^*$, $\gamma = 0.5 a^* \cdot R^*$ and $p=1$.

To investigate the effects of external parameters like Rashba and topological defect, we have plotted in Fig(3.5) the $\langle E \rangle$ against ω_c for $\omega_0=2.5 R^*$ and $T=5K$, and various selected values of Rashba parameter $\gamma = 0a^*.R^*$ and $\gamma = 0.7 a^*.R^*$, and topological p values $p=1$ and $p=1.5$.

The energy spectra show an enhancement for topological factor effect while the Rashba terms lowers the energy spectra, as we explained previously.

In figure (3.5), if we exclude the effect of γ and p ($\gamma = 0a^*.R^*$, $p=1$); we find the inflection point at $\omega_c \approx 0.8 R^*$.

When we apply the RSOI it is appearing at $\omega_c \geq 0.5 R^*$, and the energy decreases with increasing ω_c . However, the p effect appears at the same point ($\omega_c \geq 0.5 R^*$) but the energy increases with increasing ω_c .

If we apply RSOI and p , the effect of γ is higher than p until $\omega_c = 3.2R^*$ that the energy decreases. However, for $\omega_c \geq 3.2 R^*$ the p effect is higher than γ and the energy increases.

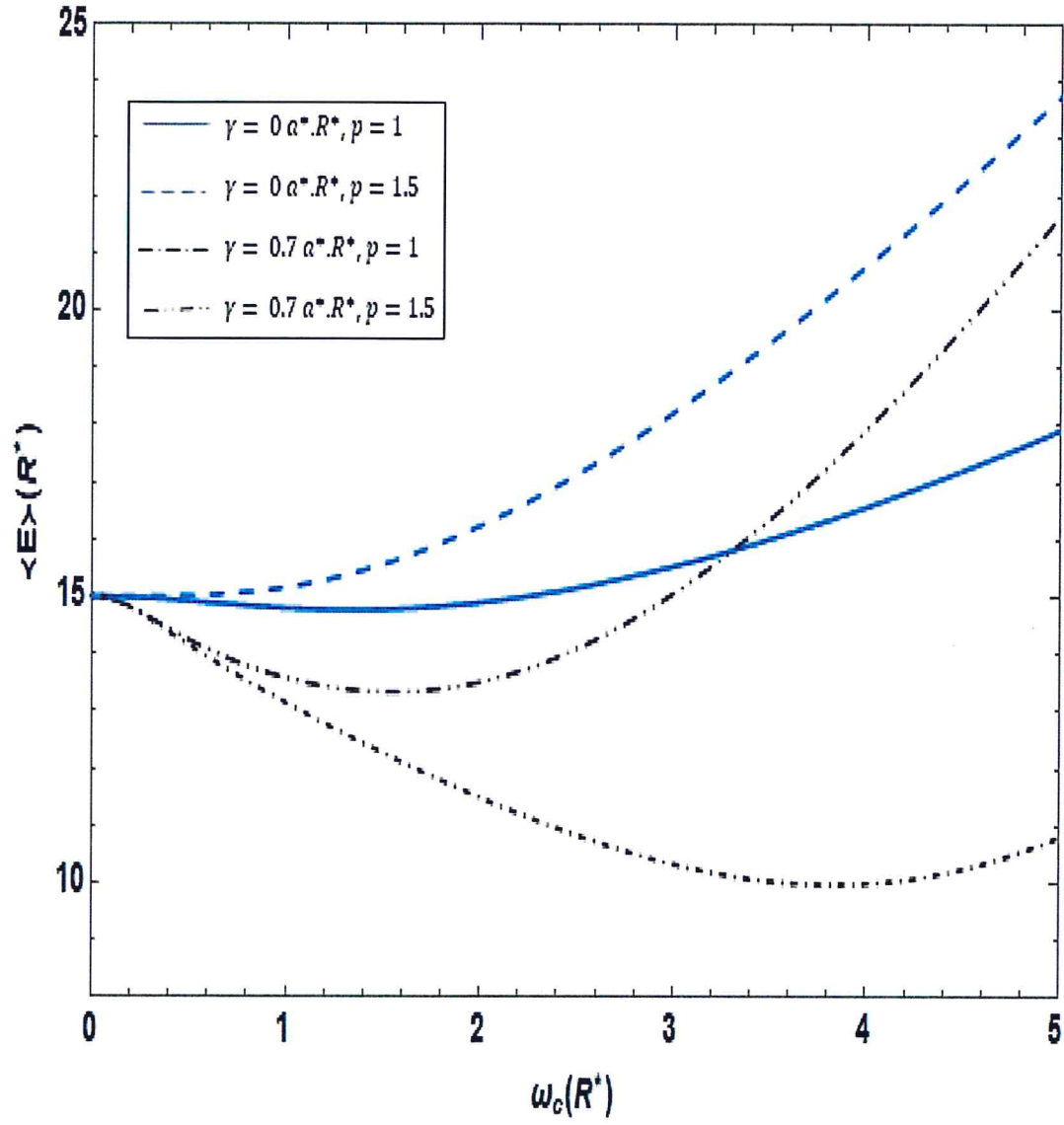


Fig (3.5): The $\langle E \rangle$ vs ω_c with $\omega_0 = 2.5 R^*$ and $T = 5K$.

In Fig. (3.6a and b), we have displayed the dependence of the average energy $\langle E \rangle$ on the temperature (T) taking into consideration the effects of Rashba and topological effects. We found in Fig. (3.6a) that the Rashba term decreases the energy as we expect. However, in Fig. (3.6b), the topological effects appear only for low ($T < 100\text{K}$) and high temperature ($T > 200\text{K}$).

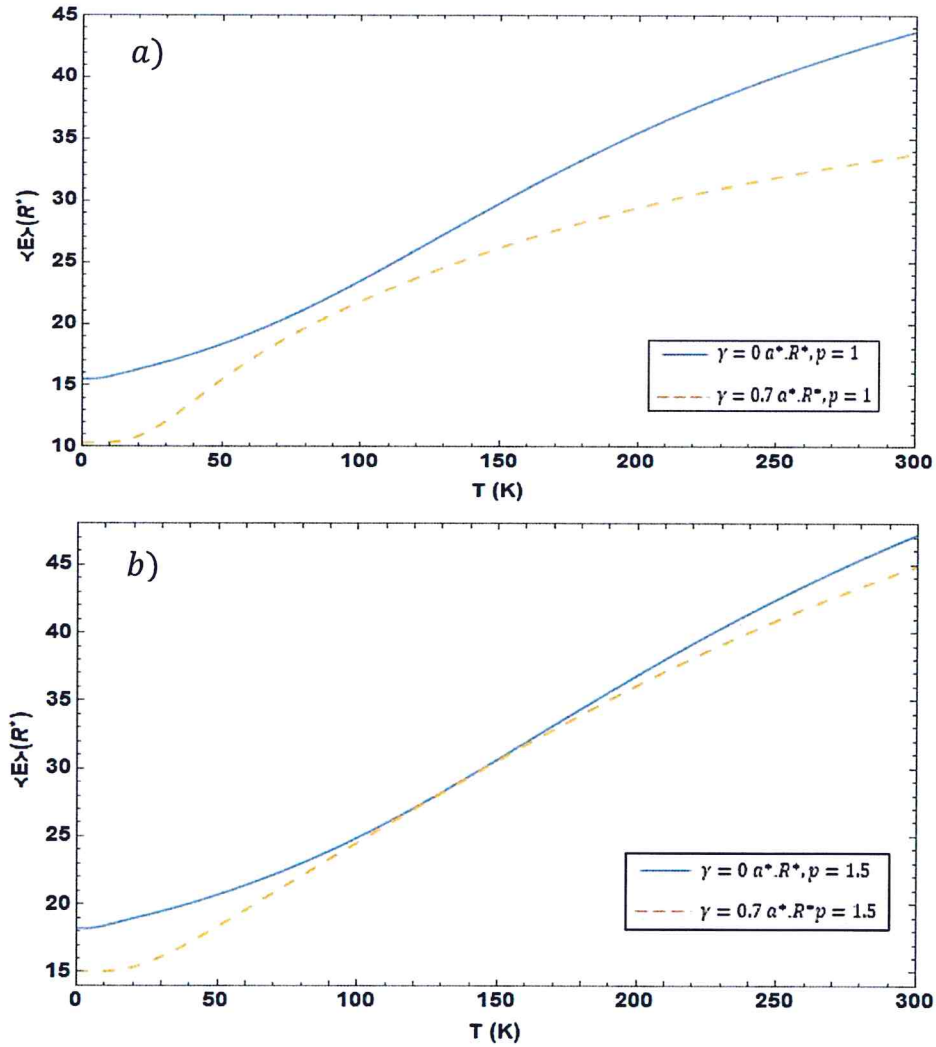


Fig (3.6): $\langle E \rangle$ vs T with $\omega_c = 3R^*$, $\omega_0 = 2.5 R^*$ and in state a) $p=1$ and b) $p=1.5$.

To demonstrate the effect of topological defect, we have plotted in Fig. (3.7a and b) again the energy spectra for fixed values of Rashba value, while varying the topological effect: $p=1$ and 1.5.

Fig. (3.7a) shows small enhancement the energy of the QD as we switch p -parameter from $p = 1$ to $p = 1.5$ and for zero Rashba effect.

For Fig. (3.7b), the case simultaneous of Rashba and topological effects, the topological defect has signification energy enhancement only for high temperature range, $T > 150\text{K}$, and small effect for low Temperature range, $T < 150\text{K}$.

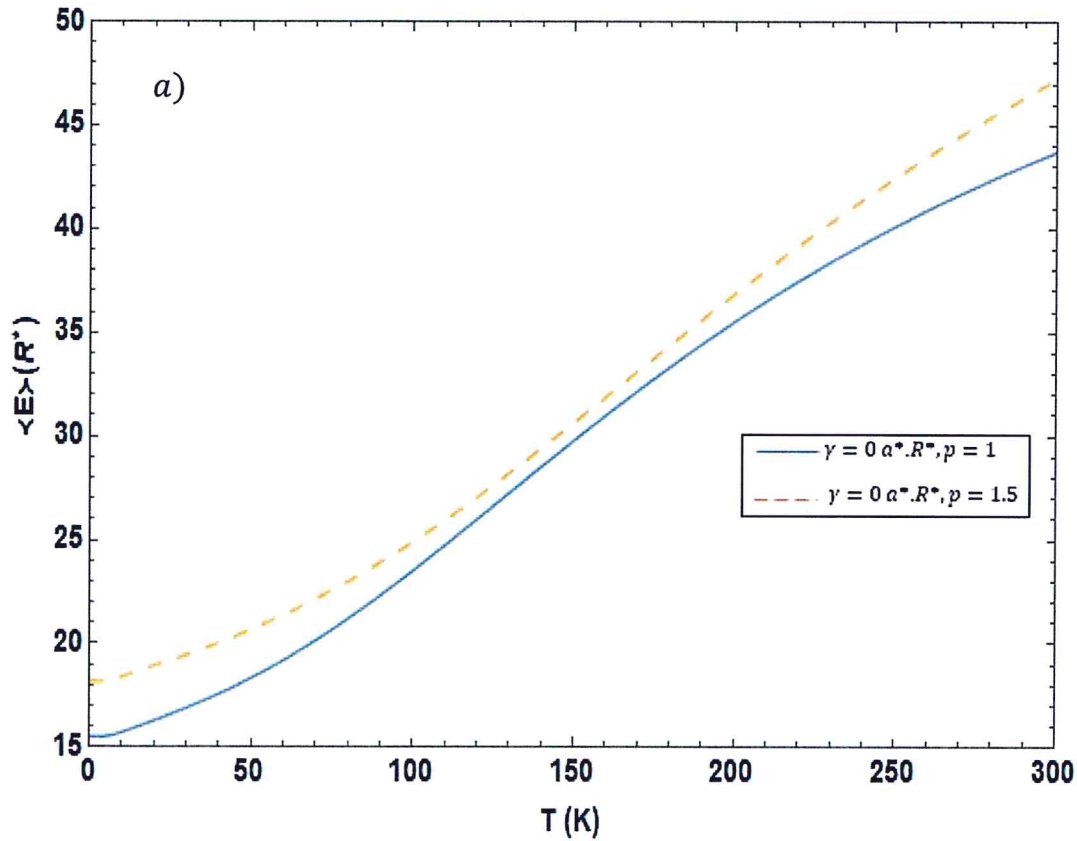


Fig (3.7): $\langle E \rangle$ vs T with $\omega_c = 3R^*$, $\omega_0 = 2.5 R^*$ and in state a) $\gamma = 0 a^*.R^*$ and b) $\gamma = 0.7 a^*.R^*$.

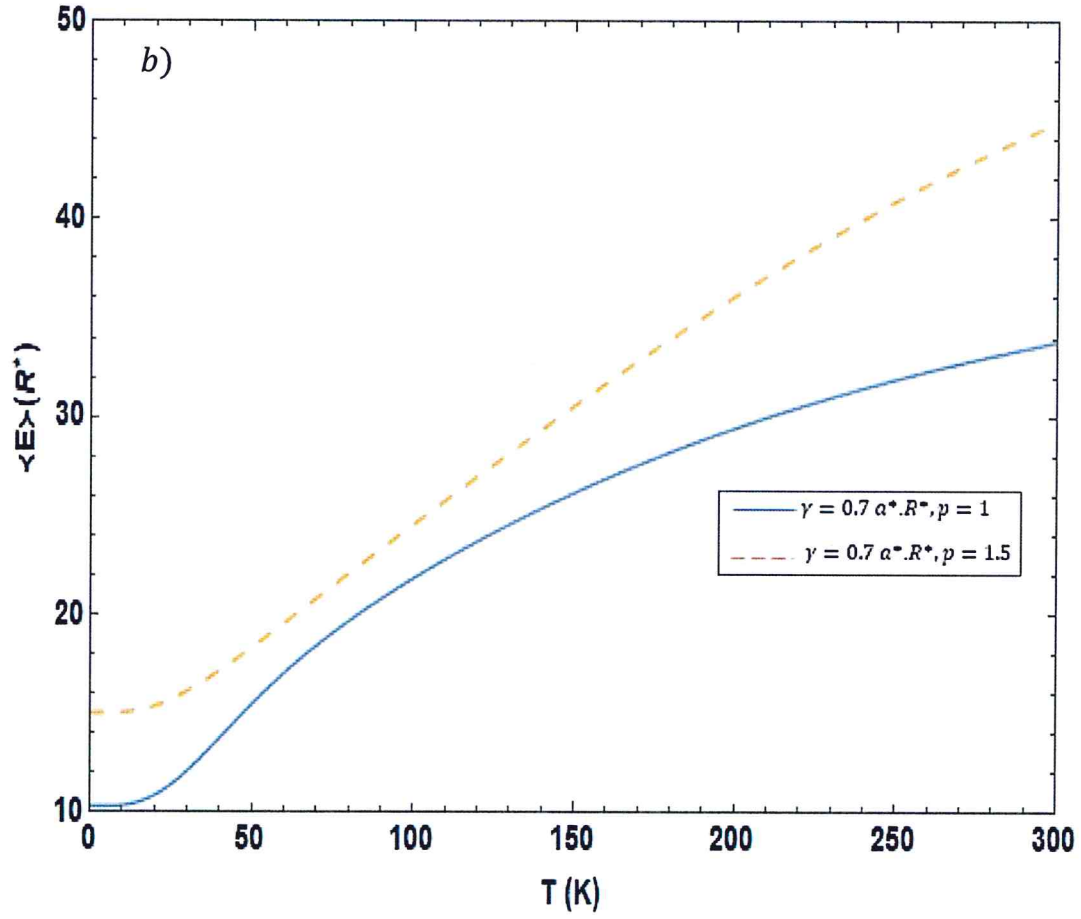


Fig. (3.7): $\langle E \rangle$ vs T with $\omega_c = 3R^*$, $\omega_0 = 2.5 R^*$ and in state *a*) $\gamma = 0 \alpha^* R^*$ and *b*) $\gamma = 0.7 \alpha^* R^*$.

3.2 Magnetic properties: Magnetization (M) and susceptibility (χ)

In this section, we discuss the computed results for magnetization and susceptibility, for all statistical energy figures shown in the previous section.

The variation of magnetization as a function of ω_c for different cases of p and γ is shown in Fig.

(3.8). When M has negative sign for the derivative of $\langle E \rangle$ with respect to ω_c , at $p=1$ and

$\gamma = 0 \alpha^*. R^*$ we see the M increases until $\omega_c \approx 0.8 R^*$ and decreases, while for $p=1.5$ its decreases after $\omega_c=0.8 R^*$, but at $\gamma = 0.7 \alpha^*. R^*$ M decreases with increasing ω_c , however, when $p=1.5$ it decreases faster than that at $p=1$.

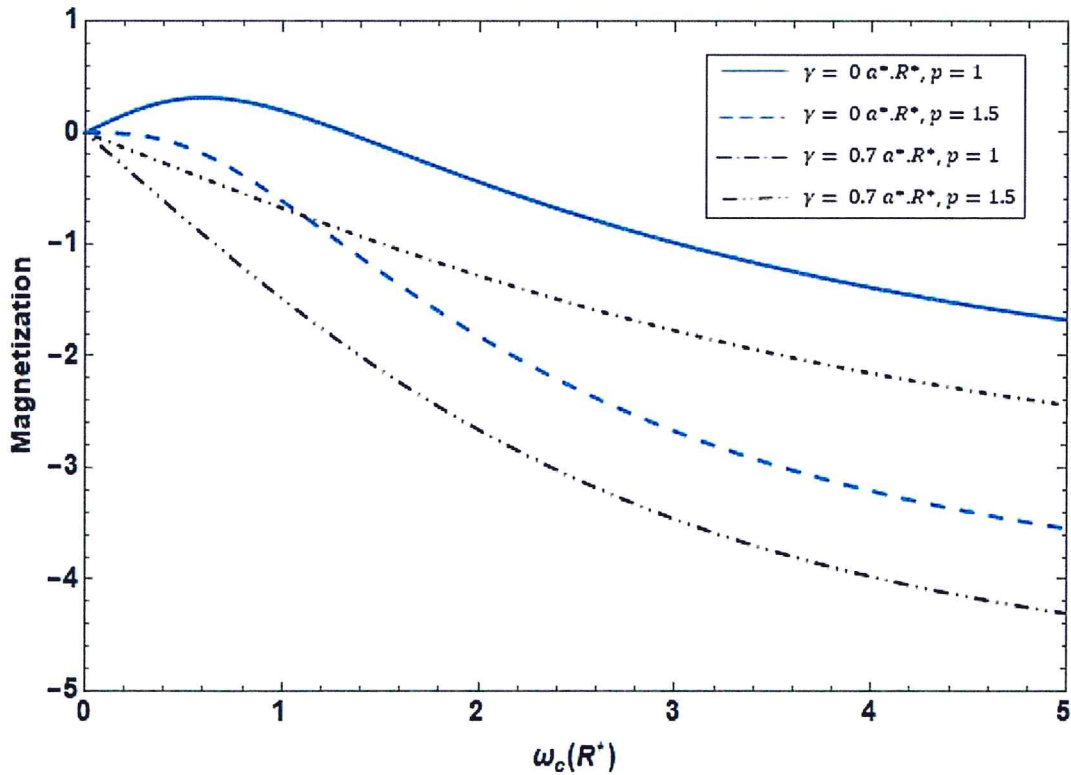


Fig (3.8): The M vs ω_c with $\omega_0 = 2.5 R^*$ and $T=5K$.

The combination of Rashba and topological effect on the magnetization of the quantum dot is investigated. In Fig. (3.9*a* and *b*), we have displayed the magnetization (M) against the temperature (T) for various $\gamma = 0, 0.7 a^*.R^*$ and $p = 1$ and 1.5 .

For $p=1$ in Fig. (3.9*a*) M decreases for $T \leq 60K$ and then starts increasing, and it shows that the Rashba term reduces the magnetization. However, at $T \geq 250K$ M is positive and $\gamma = 0.7 a^*.R^*$ is higher than $\gamma = 0 a^*.R^*$. For $p=1.5$ the magnetization (M) in Fig. (3.9*b*) decreases for $T \leq 80K$ and then increases. The magnetization (M) is lower for $\gamma = 0.7 a^*.R^*$ case and different values of p , $p = 1$ and $p = 1.5$.

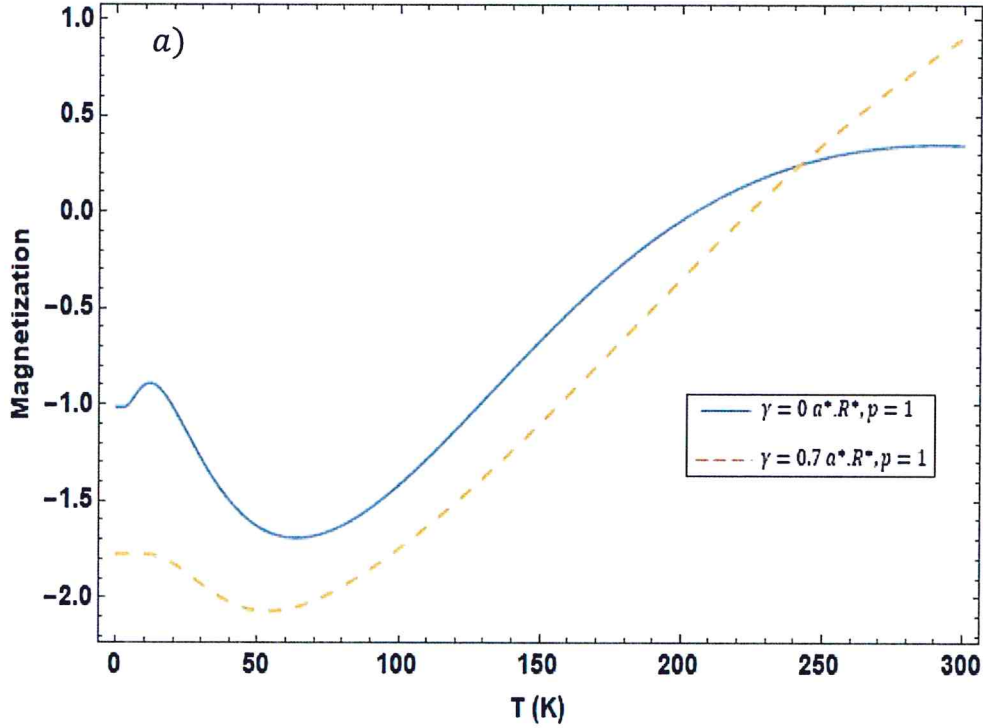


Fig. (3.9): M vs T with $\omega_c = 3R^*$, $\omega_0 = 2.5 R^*$ and in state *a*) $p=1$ and *b*) $p=1.5$.

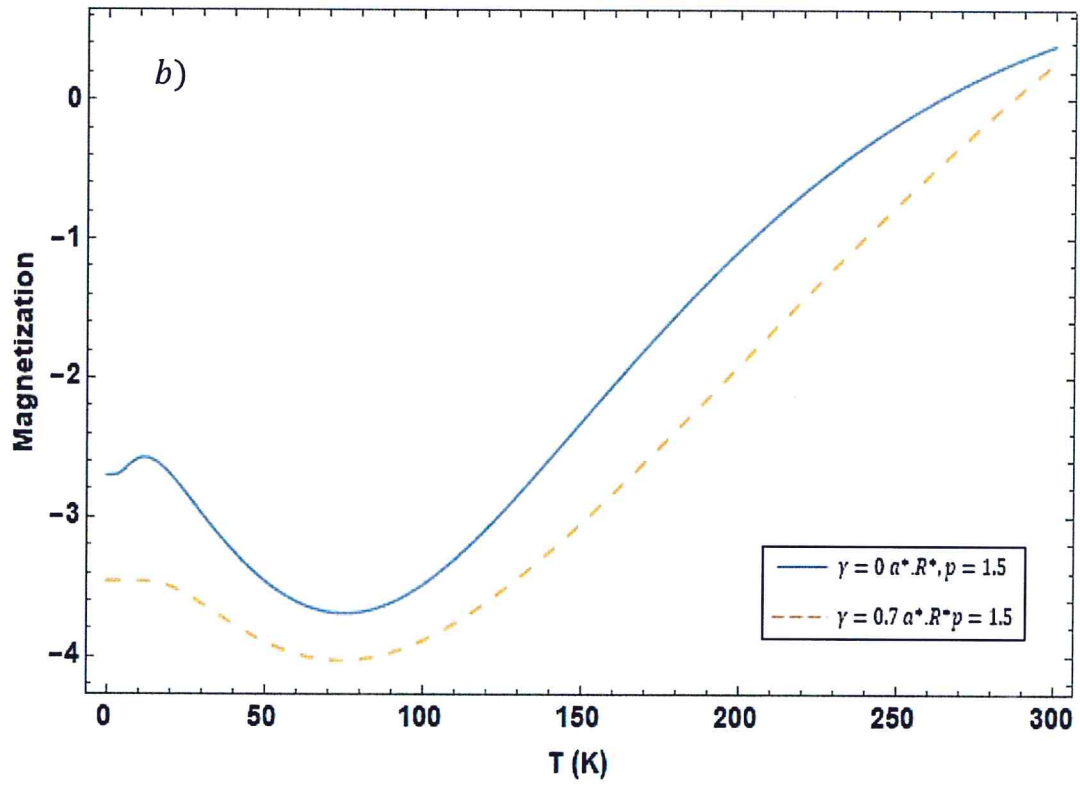


Fig. (3.9): M vs T with $\omega_c = 3R^*$, $\omega_0 = 2.5 R^*$ and in state *a*) $p=1$ and *b*) $p=1.5$.

The simultaneous of p and γ are considered. We have shown the topological effect (p) in the magnetization (M) of the QD is shown in Fig. (3.10) for absence ($\gamma = 0$) and presence the Rashba term ($\gamma = 0.7 a^* R^*$). The Figures clearly show the significant influence of the topological defect on the M in presence of γ term.

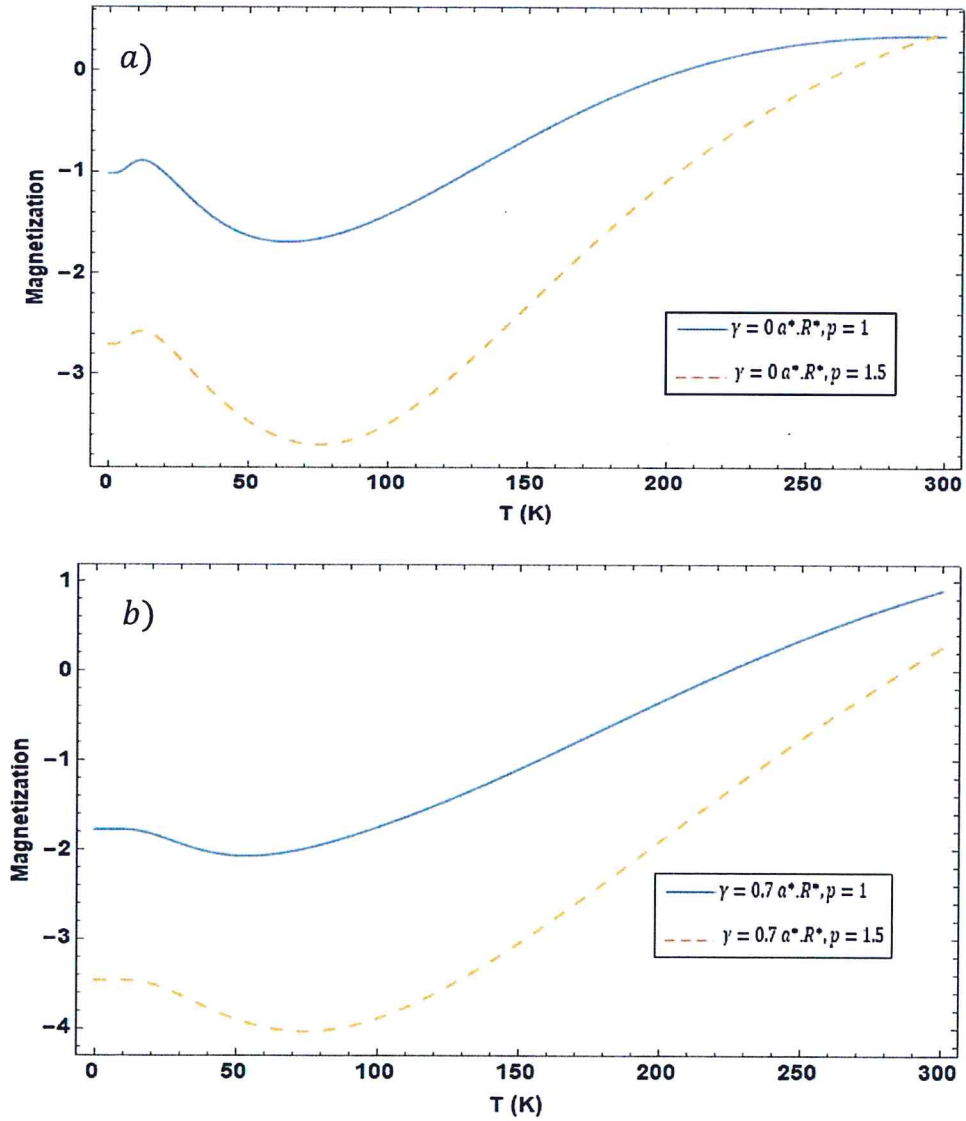


Fig (3.10): M vs T with $\omega_c = 3R^*$, $\omega_0 = 2.5 R^*$ and in state a) $\gamma = 0 a^* R^*$ and b) $\gamma = 0.7 a^* R^*$.

The variation of the susceptibility as a function of ω_c for various values of p and γ is shown in Fig. (3.11). Where χ is the derivative of $\langle E \rangle$ with respect to M .

We can see from the figure that at $p=1$ and $\gamma = 0 \alpha^*.R^*$, the magnetic susceptibility is positive ($\chi > 0$) until $\omega_c \approx 0.8 R^*$ and then it changes to negative ($\chi < 0$). This sign flipping in χ means the material can change from diamagnetic to paramagnetic. For $p=1.5$, χ is negative for all ω_c range, with Rashba coupling ($\gamma = 0.7 \alpha^*.R^*$) the material is diamagnetic.

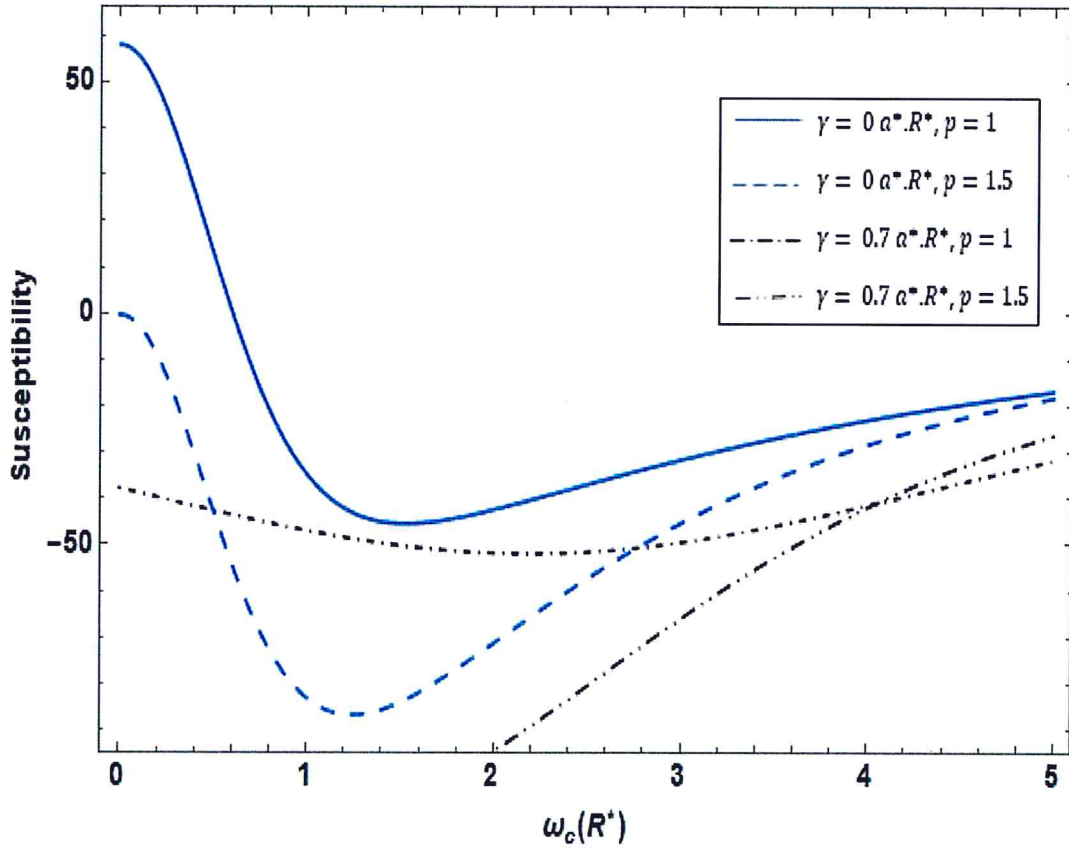


Fig. (3.11): χ vs ω_c with $\omega_0 = 2.5 R^*$ and $T=5K$.

Fig. (3.12a and b) show the effect of topological factor (p), on the magnetic susceptibility of the QD made from GaAs/AlGaAs material, with and without Rashba coupling effect.

For example, in Fig. (3.12a), the plot clearly shows the great change in the behavior of the χ curves due to the Rashba coupling ($\gamma = 0$ and $0.7 a^* R^*$) and for no p effect ($p = 1$). Fig. (3.12b) shows the behavior of χ curves for simultaneous impact of p and γ . This is consistent with the overall format in Ref. [39].

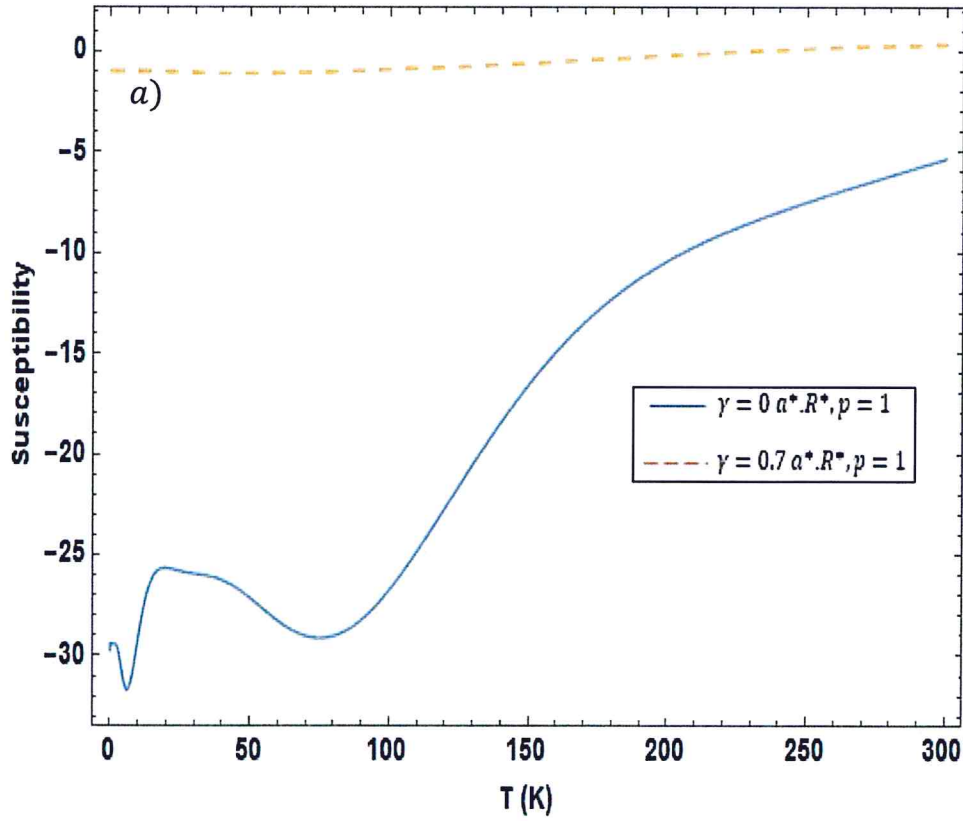


Fig (3.12): χ vs T with $\omega_c = 3R^*$, $\omega_0 = 2.5 R^*$ and in state a) $p=1$ and b) $p=1.5$.

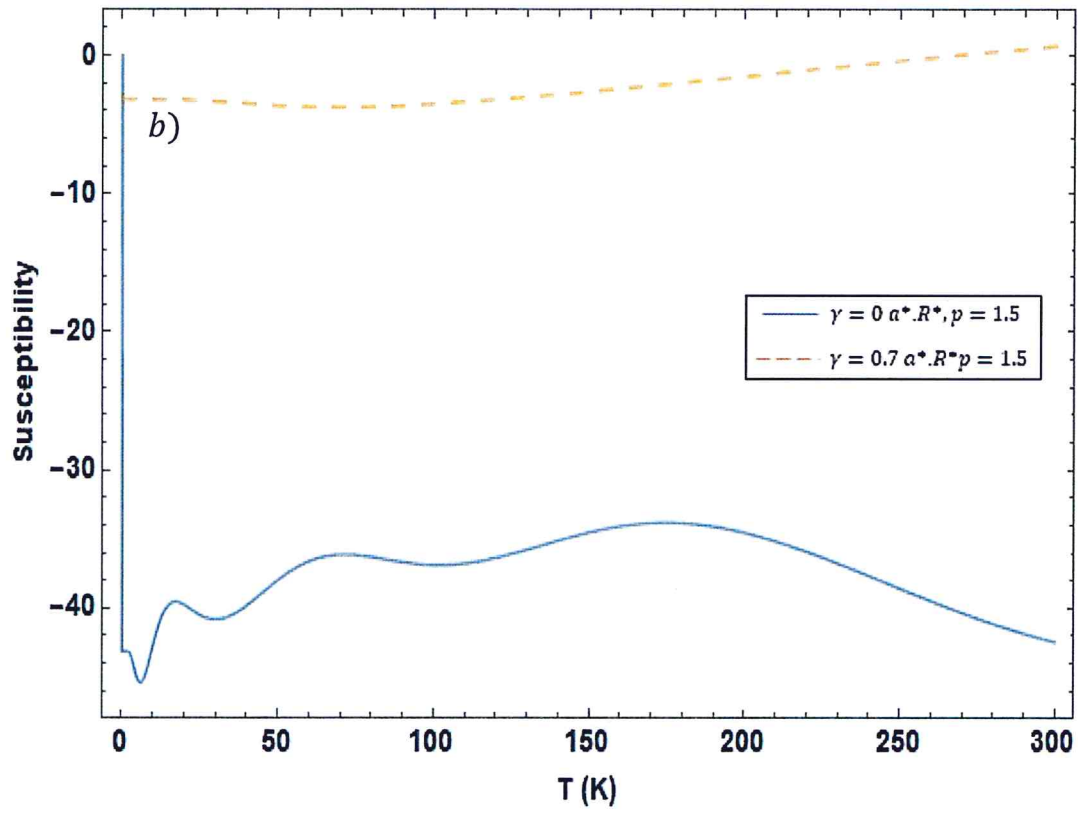


Fig (3.12): χ vs T with $\omega_c = 3R^*$, $\omega_0 = 2.5 R^*$ and in state *a*) $p=1$ and *b*) $p=1.5$.

The topological effect on thermal energy is shown in Fig. (3.13a with $\gamma = 0 a^*.R^*$ and 3.13b with $\gamma = 0.7 a^*.R^*$). In this case the temperature is another important factor that controls the magnetic type of the QD material. For Fig. (3.13a) the χ is negative.

While in Fig. (3.13b), $p=1$, $\gamma = 0.7 a^*.R^*$ and $T=150K$ the material type is changed from diamagnetic to paramagnetic as χ changes the sign from negative to positive.

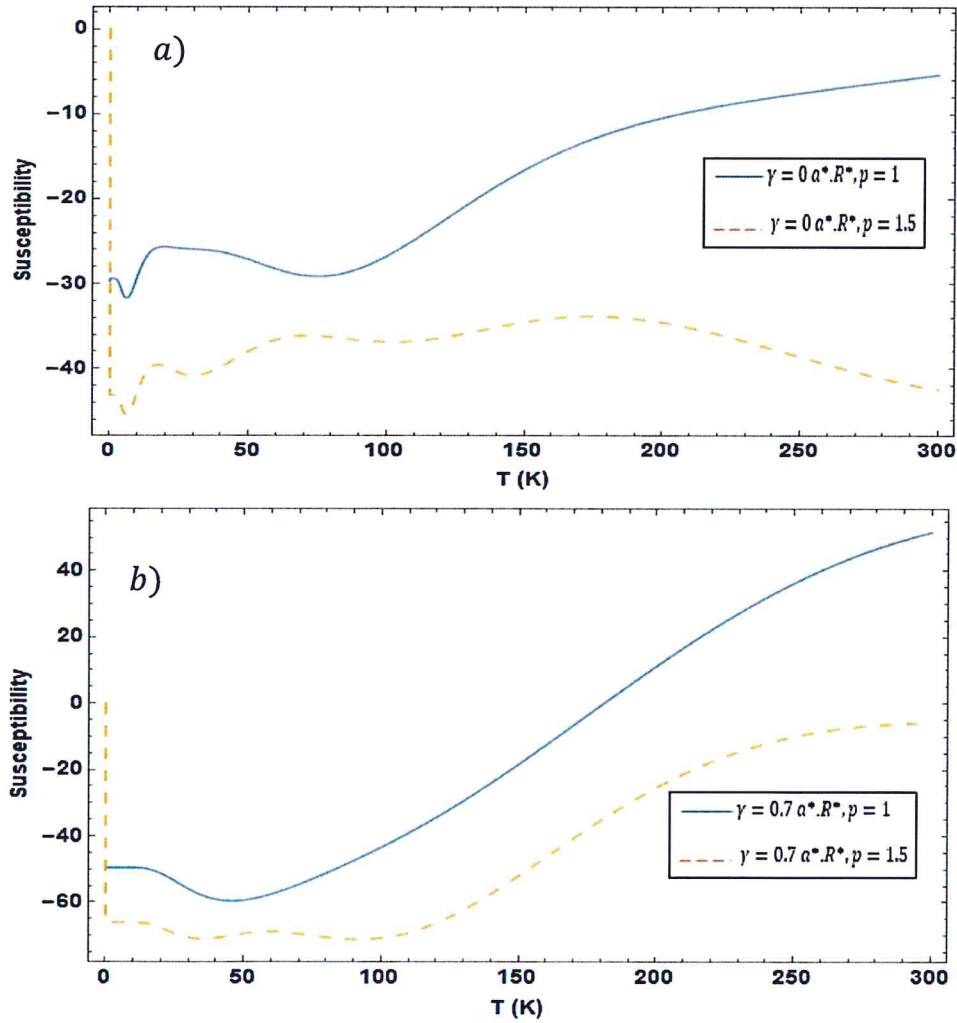


Fig (3.13): χ vs T with $\omega_c = 3R^*$, $\omega_0 = 2.5 R^*$ and in state a) $\gamma = 0 a^*.R^*$ and b) $\gamma = 0.7 a^*.R^*$.

3.3 Thermal properties: Heat capacity (C_v)

In this section, we discuss the obtained results for the heat capacity for the QD as function of various Hamiltonian physical parameters ω_c , p , γ and T .

The variation of C_v as a function of ω_c for different cases of p and γ is shown in Fig (3.14). At $\gamma = 0 \text{ } a^*.R^*$ no effect of p for C_v is observed, the heat capacity increases until $\omega_c=1.4 R^*$ and then decreases. The peak of C_v curve is found to be at $\omega_c=0.4 R^*$ for $\gamma = 0.7 \text{ } a^*.R^*$ and $p = 1$. The p factor reduces the peak in the C_v due to the enhancement in the QD. That Corresponds to the behavior of C_v in Ref. [34].

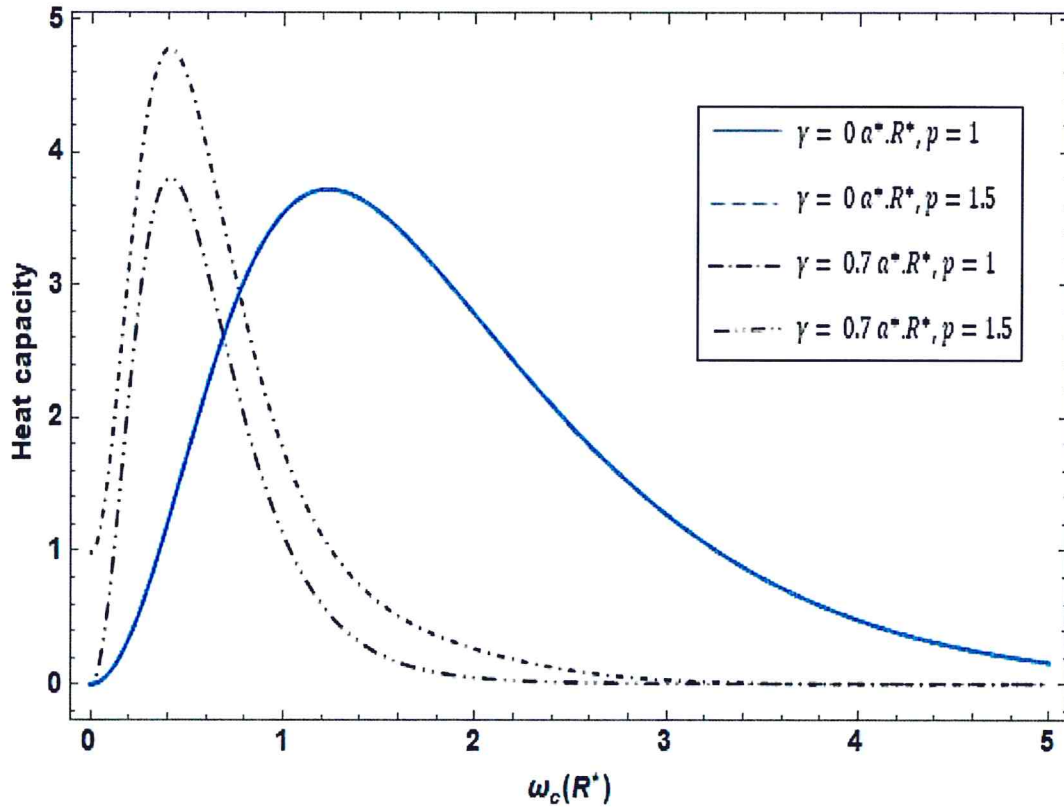


Fig (3.14): The C_v vs ω_c with $\omega_0= 2.5 R^*$ and $T=5K$.

The effect of Rashba parameter is shown in Fig. (3.15*a* and *b*) on the C_v curve of the QD for $p=1$ and 1.5. For both cases, the Rashba parameter enhances the C_v curve of the QD.

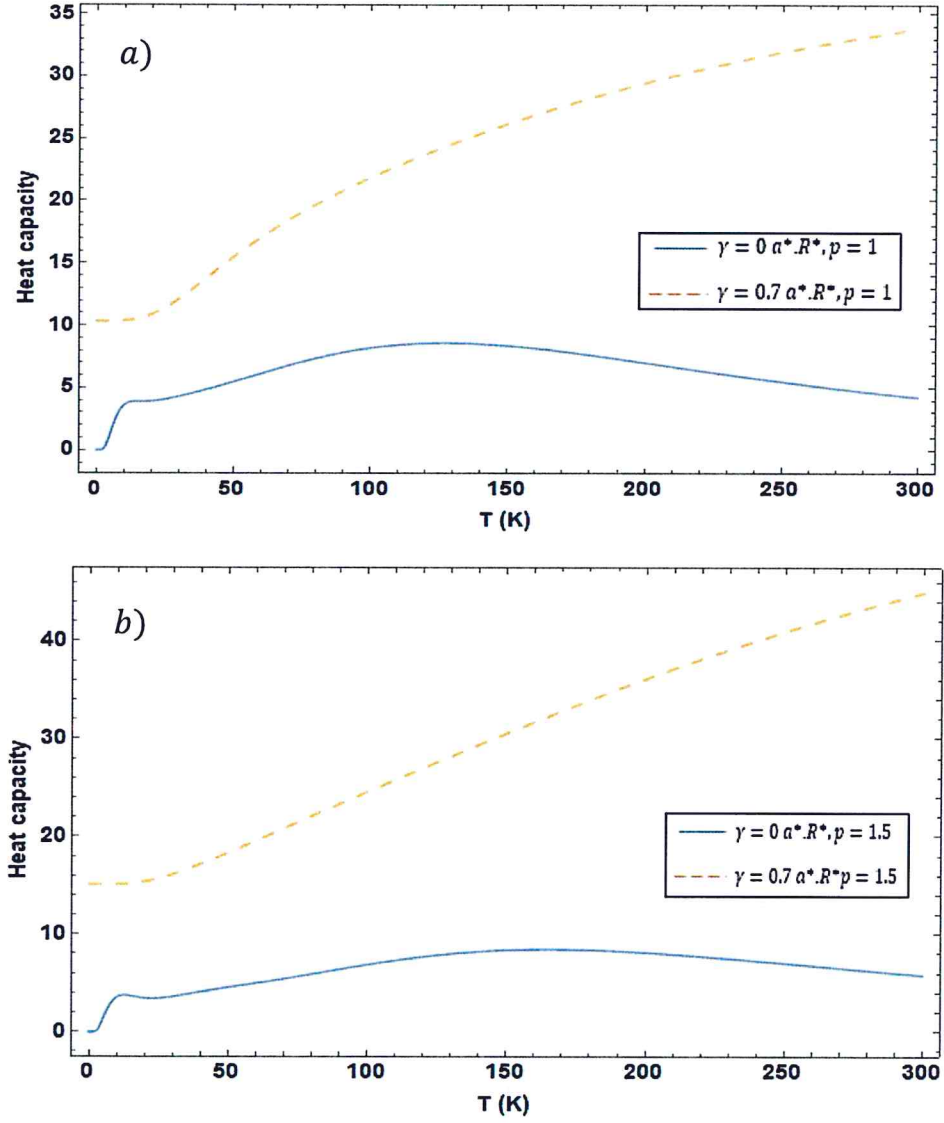


Fig (3.15): C_v vs T with $\omega_c=3R^*$, $\omega_0=2.5 R^*$ and in state *a*) $p=1$ and *b*) $p=1.5$.

In Fig. (3.16a and b), we demonstrate the influence of the impact factor p on the behavior of the C_v curve in the absence and presence of Rashba effect.

In Fig. (3.16a), we can observe the shift of the wide peak of the heat capacity, towards a higher temperature, as we increase from $p = 1$ to $p = 1.5$, and in the absence of Rashba effect ($\gamma = 0$).

However, for $\gamma = 0.7 a^* R^*$ case, Fig. (3.16b) shows a great reduction in the height of the peak curve as p increases from $p = 1$ to $p = 1.5$. In addition, the Schottky transition peak disappeared.

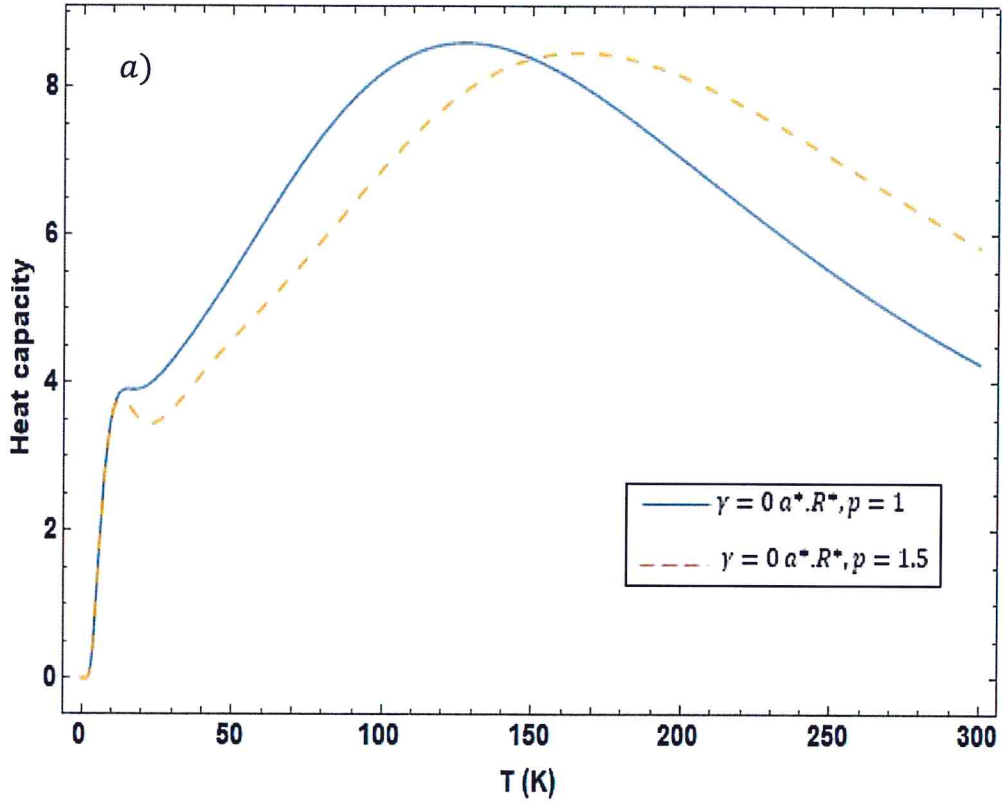


Fig. (3.16): C_v vs T with $\omega_c = 3R^*$, $\omega_0 = 2.5 R^*$ and in state a) $\gamma = 0 a^* R^*$ and b) $\gamma = 0.7 a^* R^*$.

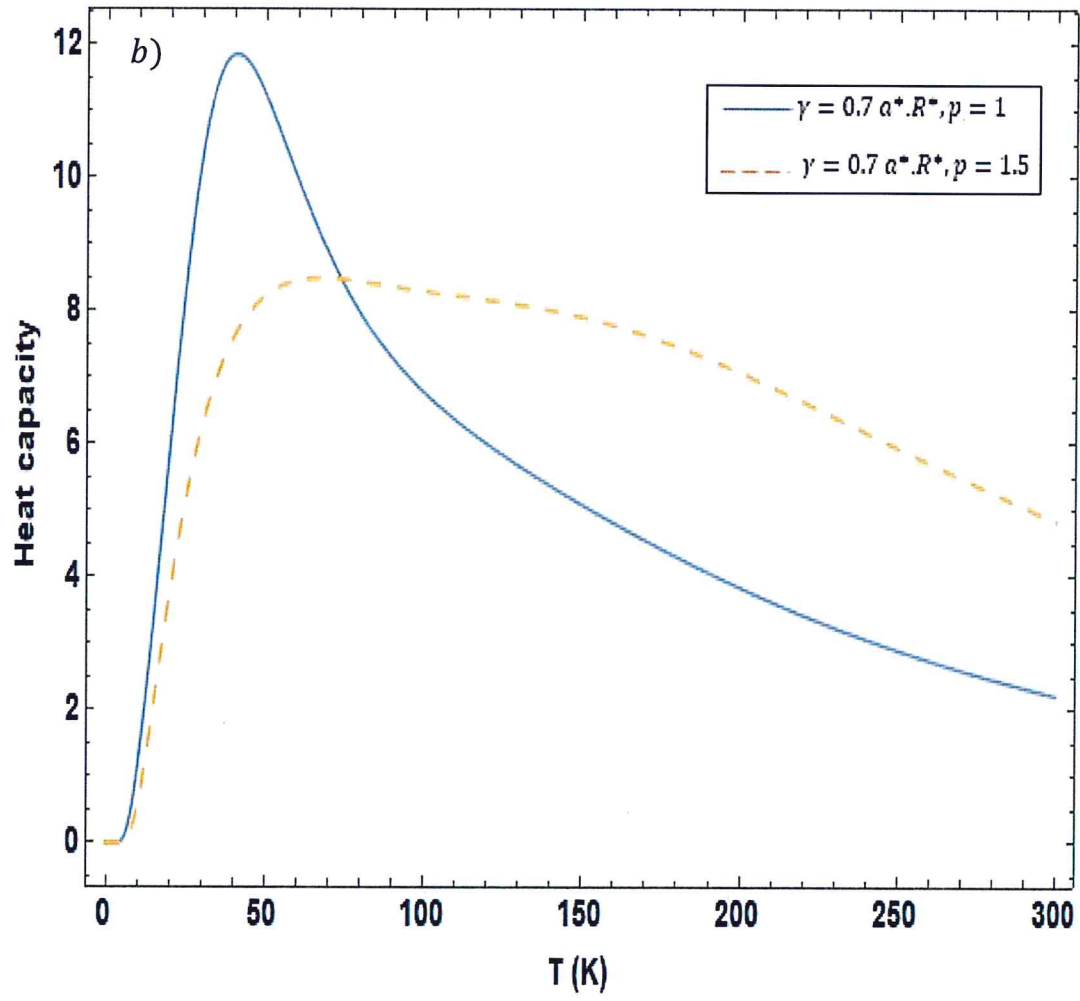


Fig. (3.16): C_v vs T with $\omega_c = 3R^*$, $\omega_0 = 2.5 R^*$ and in state a) $\gamma = 0 a^*.R^*$ and b) $\gamma = 0.7 a^*.R^*$.

3.4 Magnetic phase transition:

In this section, we search for the magnetic phase diagrams of the GaAs nanomaterial for a wide range of QD physical parameters. To achieve our objective, we present a contour-plot (Figures 3.17 to 3.20) for the magnetic susceptibility of the QD as function of the QD-physical parameters.

Figure (3.17) shows the phase transition obtained by equation (2.15), without any external affect. The obtained contour plot is in a very good agreement with the corresponding one given by R efs. [32,34].

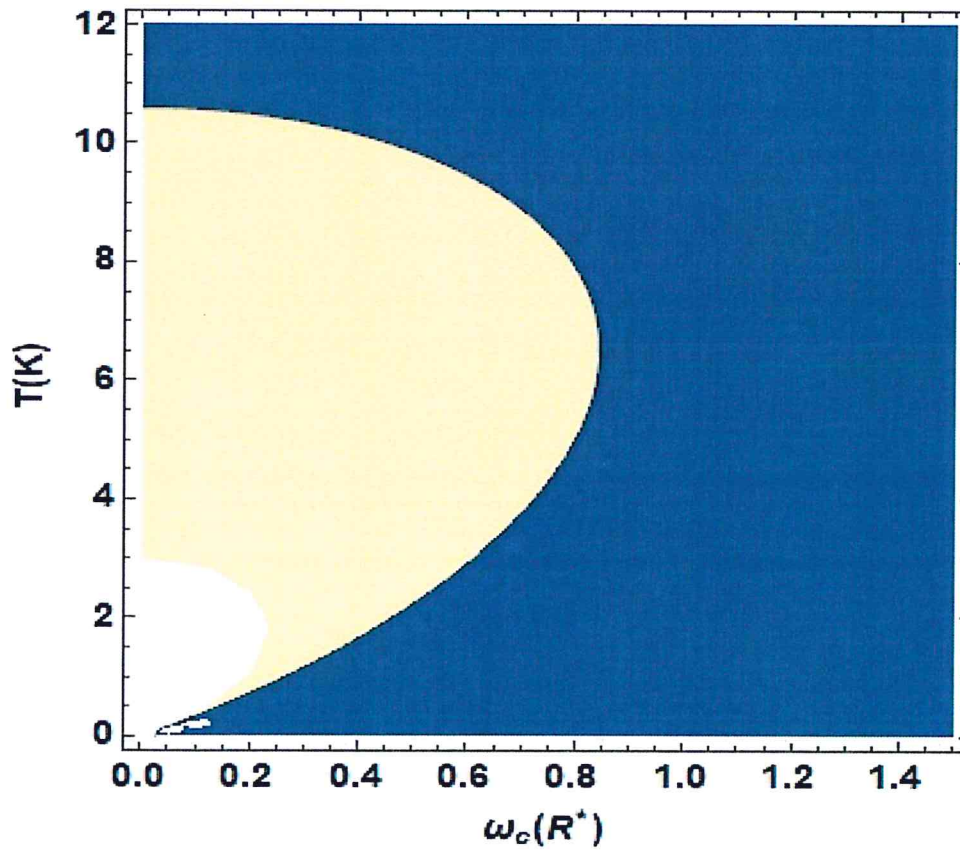


Fig. (3.17): Magnetic phase diagram of GaAs QD as a function of the temperature and magnetic field with $\omega_0 = 6.3R^*$, $p=1$ and $\gamma = 0 a^* \cdot R^*$.

Figures (3.18) to (3.20) show clearly the contour plot of quantum dot magnetic susceptibility and the magnetic phase transition. The golden region stands for the paramagnetic phase ($\chi > 0$) while the blue area for the diamagnetic phase ($\chi < 0$) of the quantum dot and for a wide range of the magnetic field, confinement, temperature, Rashba and topological parameters.

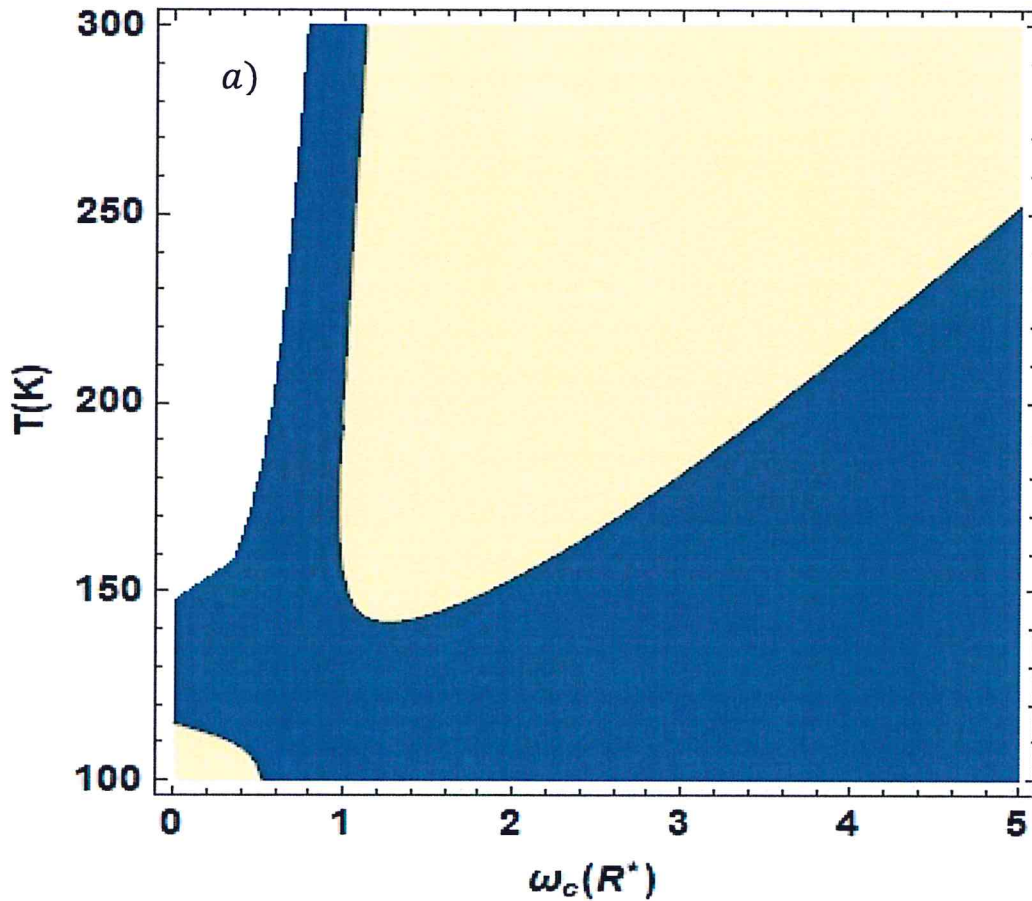
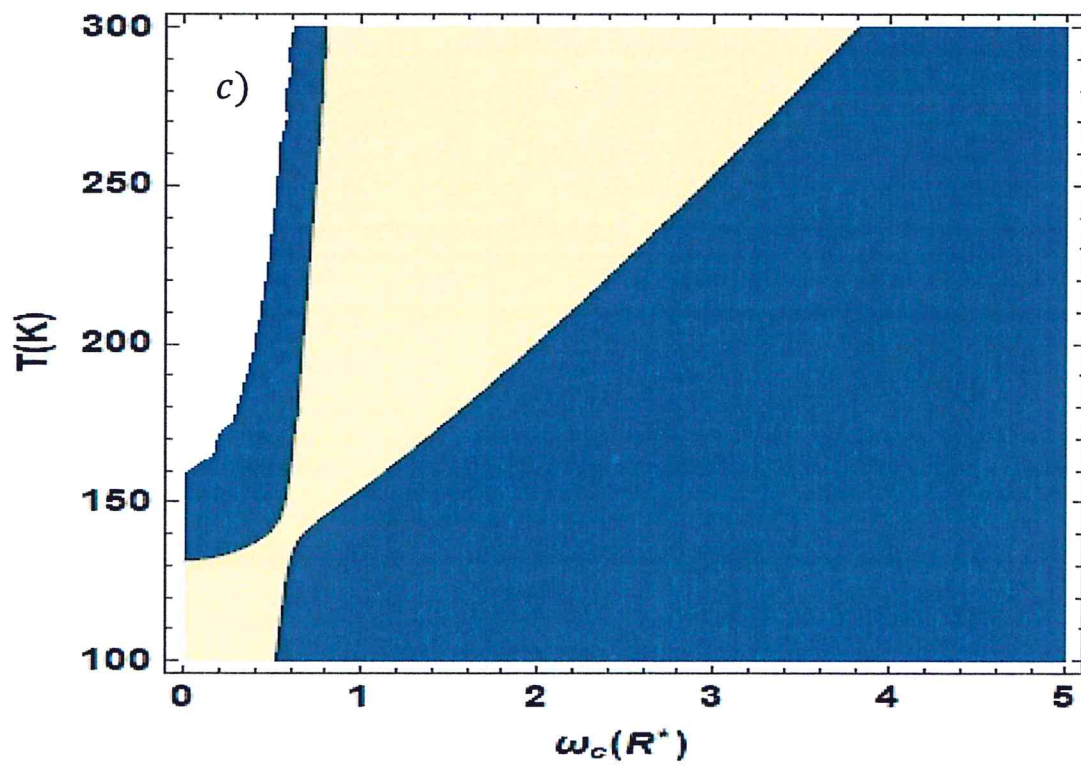
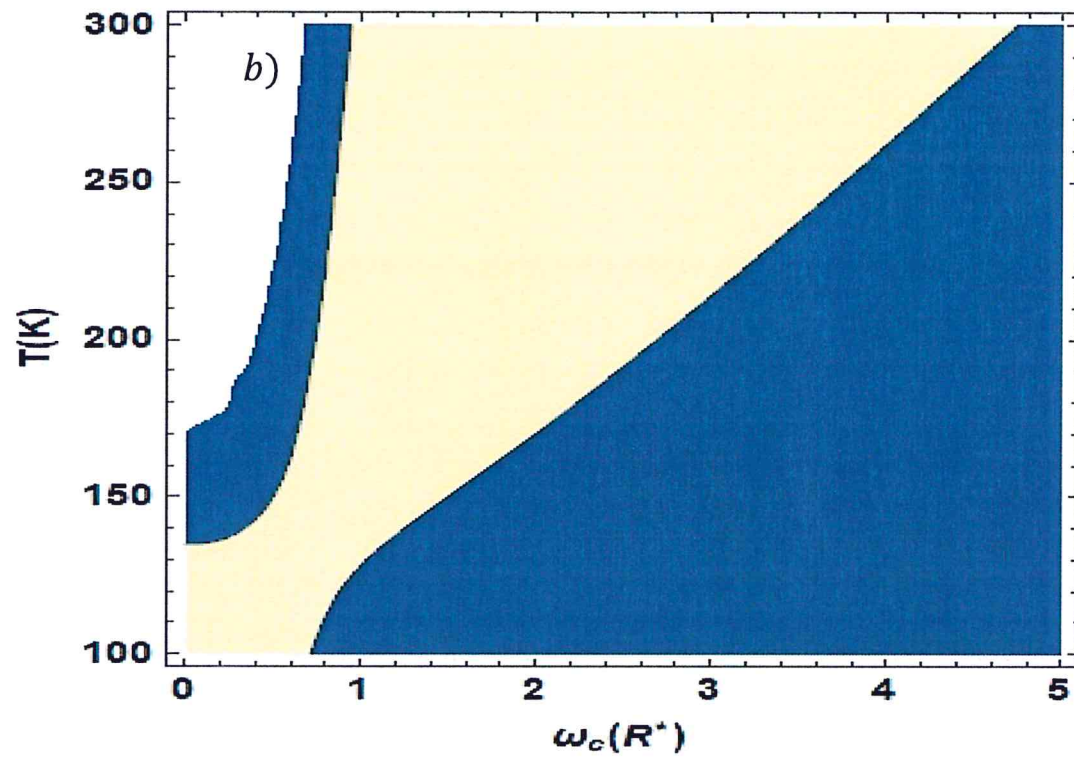


Figure (3.18): Magnetic phase diagram of GaAs QD as a function of the T and ω_c with $\omega_0 = 0.5R^*$ for a) $p=1$, $\gamma = 0 a^*.R^*$, b) $p=1$, $\gamma = 0.35 a^*.R^*$, c) $p=1.2$, $\gamma = 0 a^*.R^*$ and d) $p=1.2$ and $\gamma = 0.35 a^*.R^*$. The golden region corresponds to the paramagnetic phase ($\chi > 0$) whereas the blue region to the diamagnetic phase ($\chi < 0$).



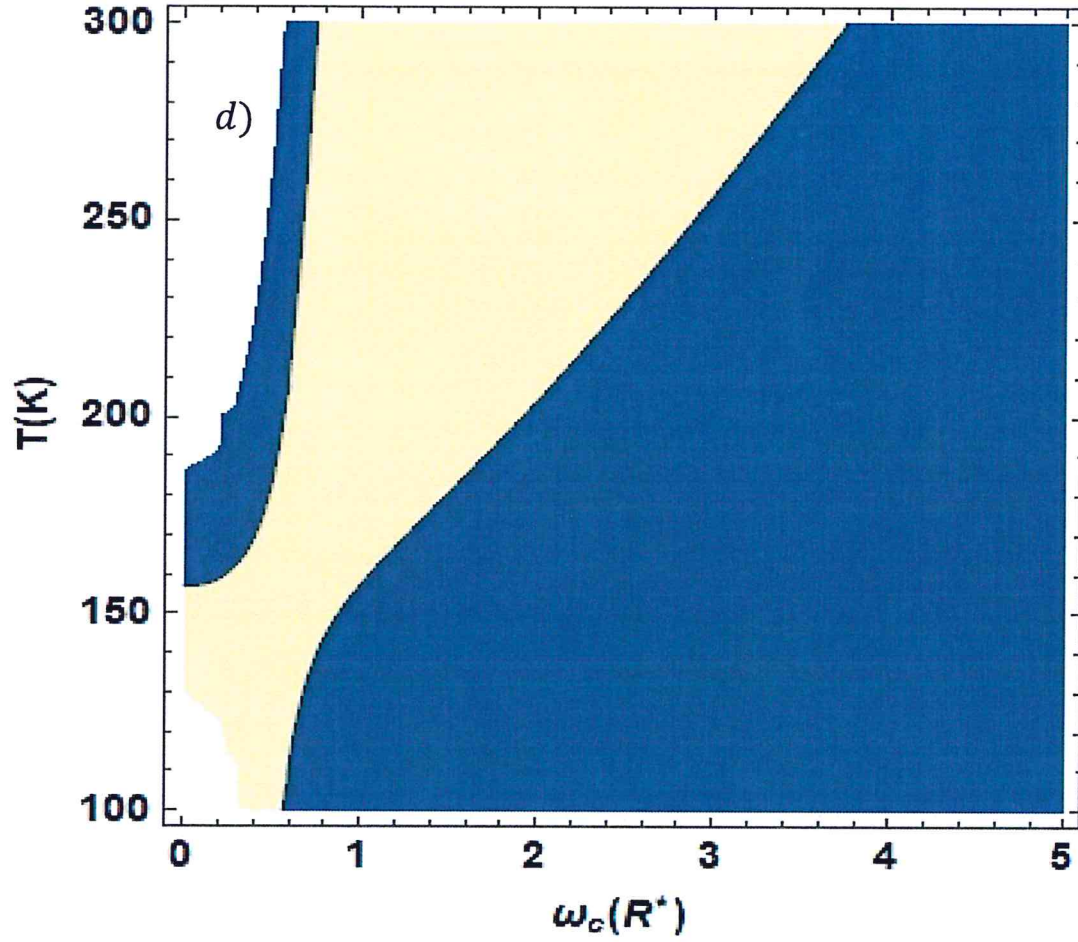


Figure (3.18): Magnetic phase diagram of GaAs QD as a function of the T and ω_c with $\omega_0 = 0.5R^*$ for *a*) $p=1$, $\gamma = 0 a^*.R^*$, *b*) $p=1$, $\gamma = 0.35 a^*.R^*$, *c*) $p=1.2$, $\gamma = 0 a^*.R^*$ and *d*) $p=1.2$ and $\gamma = 0.35 a^*.R^*$. The golden region corresponds to the paramagnetic phase ($\chi > 0$) whereas the blue region to the diamagnetic phase ($\chi < 0$).

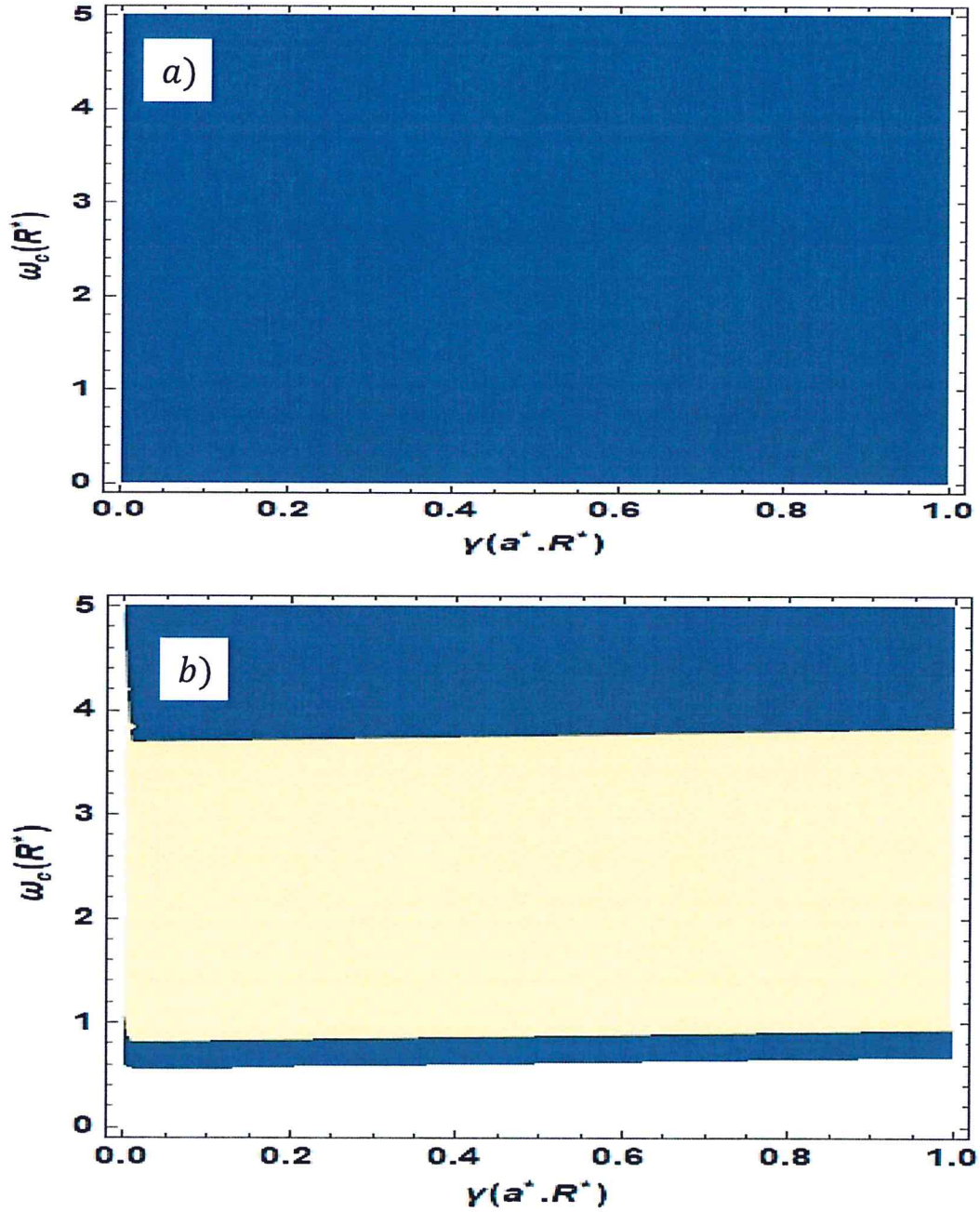


Figure (3.19): Magnetic phase diagram of GaAs QD as a function of the ω_c and γ with $\omega_0 = 0.5 R^*$ and $p=1$ for *a)* $T = 20$ K, *b)* $T = 250$ K. The golden region corresponds to the paramagnetic phase ($\chi > 0$) whereas the blue region to the diamagnetic phase ($\chi < 0$).

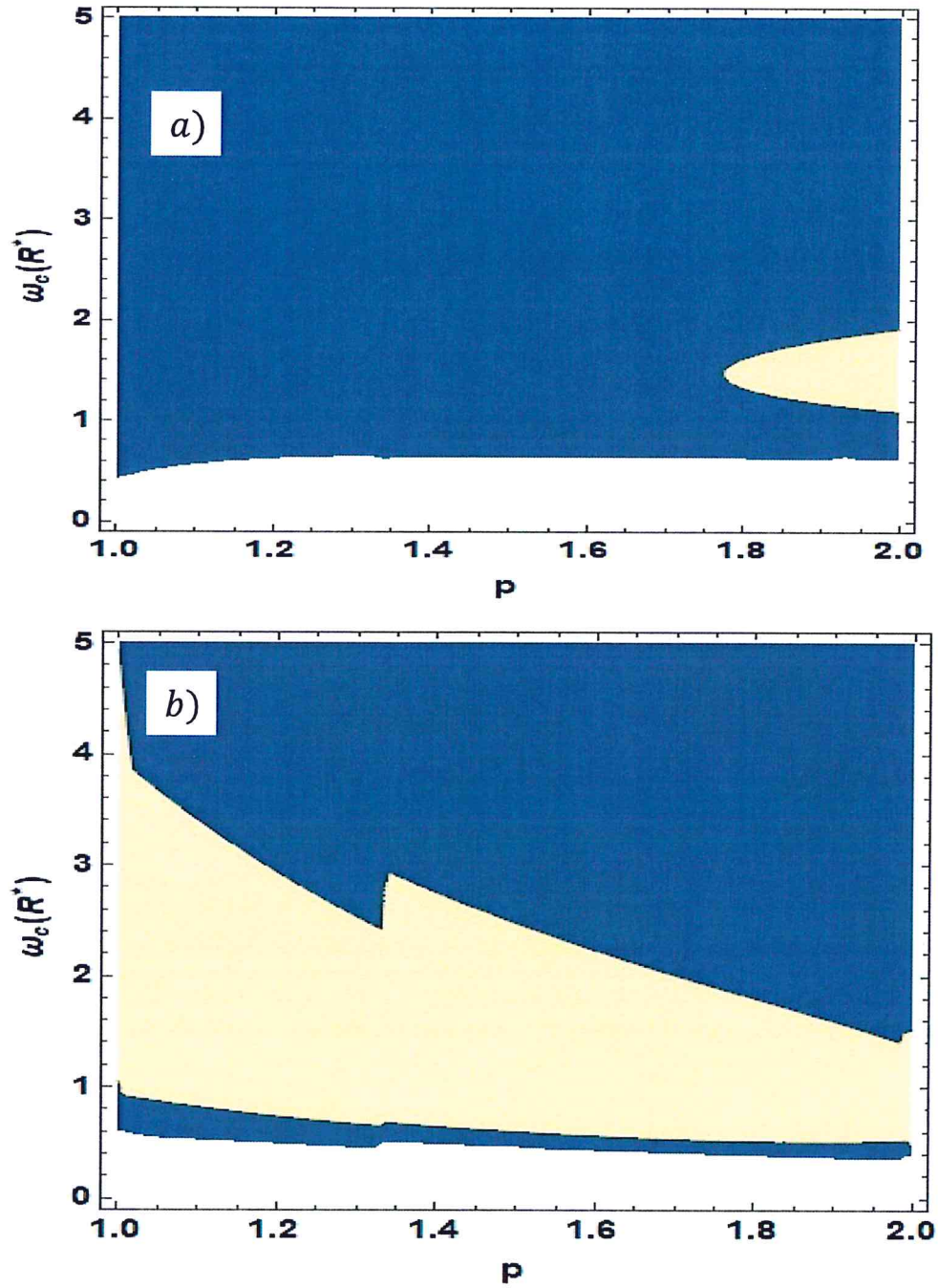


Figure (3.20): Magnetic phase diagram of GaAs QD as a function of the ω_c and p with $\omega_0 = 0.5R^*$ and $\gamma = 0$ a*. R^* for a) $T = 20$ K, b) $T = 250$ K. The golden region corresponds to the paramagnetic phase ($\chi > 0$) whereas the blue region to the diamagnetic phase ($\chi < 0$).

Chapter Four

Conclusion and Future work

In this study, the Hamiltonian of a single electron confined in a parabolic quantum dot in the presence of Rashba spin orbit interaction term effect, applied uniform magnetic field and topological defect had been reproduced by analytical method.

We have studied the dependence of the energy spectrum for our QD as a function

of: confinement frequency (ω_0), magnetic field (ω_c), Rashba (γ) and topological parameters (p) to calculate the energy spectra. Our results are in good agreement with reported works.

Moreover, the statistical energy spectra $\langle E \rangle$ and the magnetic properties like; Magnetization (M) and Magnetic susceptibility (χ) were computed as a function of our quantum dot physical parameters ($\omega_0, \omega_c, p, \gamma, T$). It was found that, as we increase the Rashba term (γ) the energy spectra of the QD is significantly decreases, this enhancement in the energy spectra affected greatly the magnetic properties of the QD like M and χ .

In addition, we have studied the effect of topological defect on the energy spectra of the QD, our computed results show that if we increase the topological factor (p), the $\langle E \rangle$ increases also and this result affects M and χ .

The behavior of the magnetic susceptibility χ is shown as function of QD parameters values. We found that the QD material changes its magnetic phase from diamagnetic to paramagnetic type. These magnetic transition phase diagrams of the QD are shown explicitly in the contour plots. Furthermore, the thermal properties of the QD has been investigated. We have shown the

dependence of heat capacity (C_v) on γ and p . It was found that, as we increase the Rashba Spin Orbit Interaction parameter (γ) and the topological defect (p), the heat capacity (C_v) is enhanced for all ranges of the temperature (T).

We are planning in the future to continue our research efforts in investigating the effect of these parameters on another interesting QD properties like density of state (DOS) and in the field of Spintronics.

References:

1. Harrison, P., & Valavanis, A. (2016). *Quantum wells, wires and dots: theoretical and computational physics of semiconductor nanostructures*. John Wiley & Sons.
2. Shah, S. H. (2007). *Study of nonlinear optical properties of indium arsenide/gallium arsenide and indium gallium arsenide/gallium arsenide self-assembled quantum dots*. University of Delaware.
3. Pedersen, T. G. (2017). Stark effect in finite-barrier quantum wells, wires, and dots. *New Journal of Physics*, 19(4), 043011.
4. Tiwari, S., Rana, F., Chan, K., Shi, L., & Hanafi, H. (1996). Single charge and confinement effects in nano-crystal memories. *Applied Physics Letters*, 69(9), 1232-1234.
5. Bahramiyan, H., & Khordad, R. (2014). Effect of various factors on binding energy of pyramid quantum dot: pressure, temperature and impurity position. *Optical and Quantum Electronics*, 46(5), 719-729.
6. Xie, W. (2008). Binding energy of an off-center hydrogenic donor in a spherical Gaussian quantum dot. *Physica B: Condensed Matter*, 403(17), 2828-2831.
7. Khordad, R., & Bahramiyan, H. (2015). Impurity position effect on optical properties of various quantum dots. *Physica E: Low-dimensional Systems and Nanostructures*, 66, 107-115.

8. Kouwenhoven, L., & Marcus, C. (1998). Quantum dots. *Physics World*, 11(6), 35.
9. Toropov, A. A., Shubina, T. V., Belyaev, K. G., Ivanov, S. V., Kop'ev, P. S., Ogawa, Y., & Minami, F. (2011). Enhancement of excitonic emission in semiconductor heterostructures due to resonant coupling to multipole plasmon modes in a gold particle. *Physical Review B*, 84(8), 085323.
10. Lutchyn, R. T., Bakkers, E. P. A. M., Kouwenhoven, L. P., Krogstrup, P., Marcus, C. M., & Oreg, Y. (2018). Majorana zero modes in superconductor–semiconductor heterostructures. *Nature Reviews Materials*, 3(5), 52-68.
11. Christians, J. A., Fung, R. C., & Kamat, P. V. (2013). An inorganic hole conductor for organo-lead halide perovskite solar cells. Improved hole conductivity with copper iodide. *Journal of the American Chemical Society*, 136(2), 758-764.
12. Jamieson, T., Bakhshi, R., Petrova, D., Pocock, R., Imani, M., & Seifalian, A. M. (2007). Biological applications of quantum dots. *Biomaterials*, 28(31), 4717-4732.
13. Reshma, V. G., & Mohanan, P. V. (2019). Quantum dots: Applications and safety consequences. *Journal of Luminescence*, 205, 287-298.
14. Darawshi, A. (2018). *Effect of Applied Fields on The Magnetic Properties of Donor Impurity Confined in Parabolic GaAs Quantum Dot* (Thesis, An-Najah National University).
15. Li, C., Cheng, Y., Li, B., Cheng, F., Li, L., Qi, T., ... & Gao, Y. (2019). Study of Charge Distributions and Electrical Properties in GaAs/AlGaAs Single Quantum Well/Nanowire Heterostructure. *The Journal of Physical Chemistry C*.

16. Baghdasaryan, D. A., Hayrapetyan, D. B., Kazaryan, E. M., & Sarkisyan, H. A. (2018). Thermal and magnetic properties of electron gas in toroidal quantum dot. *Physica E: Low-dimensional Systems and Nanostructures*, 101, 1-4.
17. Nammas, F. S. (2018). Thermodynamic properties of two electrons quantum dot with harmonic interaction. *Physica A: Statistical Mechanics and its Applications*, 508, 187-198.
18. Antil, S., Kumar, M., Lahon, S., & Maan, A. S. (2019). Pressure dependent optical properties of quantum dot with spin orbit interaction and magnetic field. *Optik*, 176, 278-286.
19. Castaño-Yepes, J. D., Amor-Quiroz, D. A., Ramirez-Gutierrez, C. F., & Gómez, E. A. (2019). Impact of a topological defect and Rashba spin-orbit interaction on the thermo-magnetic and optical properties of a 2D semiconductor quantum dot with Gaussian confinement. *Physica E: Low-dimensional Systems and Nanostructures*, 109, 59-66.
20. Kumar, D. S., Mukhopadhyay, S., & Chatterjee, A. (2016). Magnetization and susceptibility of a parabolic InAs quantum dot with electron–electron and spin–orbit interactions in the presence of a magnetic field at finite temperature. *Journal of Magnetism and Magnetic Materials*, 418, 169-174.
21. Avetisyan, S., Chakraborty, T., & Pietiläinen, P. (2016). Magnetization of interacting electrons in anisotropic quantum dots with Rashba spin–orbit interaction. *Physica E: Low-dimensional Systems and Nanostructures*, 81, 334-338.

22. Xu, X., Zhuang, J., & Wang, X. (2008). SnO₂ quantum dots and quantum wires: controllable synthesis, self-assembled 2D architectures, and gas-sensing properties. *Journal of the American Chemical Society*, 130(37), 12527-12535.
23. Elsaid, M. K., & Hijaz, E. (2017). Magnetic Susceptibility of Coupled Double GaAs Quantum Dot in Magnetic Fields. *Acta Physica Polonica, A.*, 131(6).
24. Hijaz, E. (2016). *The Magnetization of The (GaAs) Double Quantum Dots in a Magnetic Field* (Thesis, An-Najah National University).
25. Shaer, A., ELSAID, M., & Elhasan, M. (2016). The magnetic properties of a quantum dot in a magnetic field. *Turkish Journal of Physics*, 40(3), 209-218.
26. Elsaid, M., Hjaz, E., & Shaer, A. (2017). Energy states and exchange energy of coupled double quantum dot in a magnetic field. *International Journal of Nano Dimension*, 8(1), 1-8.
27. El-Said, M. (1994). The magnetoabsorption spectra of donors in a quantum well wire. *Semiconductor science and technology*, 9(10), 1787.
28. Shaer, A., Elsaid, M. K., & Elhasan, M. (2016). Magnetization of GaAs parabolic quantum dot by variation method. *J. Phys. Sci. Appl*, 6(2), 39-46.
29. El-Said, M. (1998). The energy level ordering in two-electron quantum dot spectra. *Superlattices and microstructures*, 23(6), 1237-1243.
30. Elsaid, M. (2002). The spectral properties of two interacting electrons in a quantum dot. *Turkish Journal of Physics*, 26(5), 331-340.
31. El-Said, M. (1996). Ground-state properties of quantum dots with a magnetic field. *physica status solidi (b)*, 193(1), 105-111.

32. Boyacioglu, B., & Chatterjee, A. (2012). Dia-and paramagnetism and total susceptibility of GaAs quantum dots with Gaussian confinement. *Physica E: Low-dimensional Systems and Nanostructures*, 44(9), 1826-1831.
33. Chakraborty, T., & Pietiläinen, P. (2005). Electron correlations in a quantum dot with Bychkov-Rashba coupling. *Physical Review B*, 71(11), 113305.
34. Sari, H., Kasapoglu, E., Sakiroglu, S., Sökmen, I., & Duque, C. A. (2019). Impurity-related optical response in a 2D and 3D quantum dot with Gaussian confinement under intense laser field. *Philosophical Magazine*, 1-23.
35. Kumar, D. S., Mukhopadhyay, S., & Chatterjee, A. (2016). Magnetization and susceptibility of a parabolic InAs quantum dot with electron–electron and spin–orbit interactions in the presence of a magnetic field at finite temperature. *Journal of Magnetism and Magnetic Materials*, 418, 169-174.
36. Boyacioglu, B., & Chatterjee, A. (2012). Heat capacity and entropy of a GaAs quantum dot with Gaussian confinement. *Journal of applied physics*, 112(8), 083514.
37. Avetisyan, S., Pietiläinen, P., & Chakraborty, T. (2012). Strong enhancement of Rashba spin-orbit coupling with increasing anisotropy in the Fock-Darwin states of a quantum dot. *Physical Review B*, 85(15), 153301.
38. Busch, P., Heinonen, T., & Lahti, P. (2007). Heisenberg's uncertainty principle. *Physics reports*, 452(6), 155-176.

39. Castaño-Yepes, J. D., Ramírez-Gutierrez, C. F., Correa-Gallego, H., & Gómez, E. A. (2018). A comparative study on heat capacity, magnetization and magnetic susceptibility for a GaAs quantum dot with asymmetric confinement. *Physica E: Low-dimensional Systems and Nanostructures*, 103, 464-470.

الملخص

قمنا بحساب أطياف الطاقة في دالة هاملتون لإلكترون وحيد محصور في نقطة كمية ذات قطع مكافئ بوجود تأثير تفاعل رشبا المغزلي والدوراني والمجال المغناطيسي المنتظم وتأثير عيوب طوبولوجي وحلها في نموذج معين. أطياف الطاقة في النقطة الكمية استخدمت في حساب المتوسط الإحصائي للطاقة، ومن ثم تم الحصول على الكميات الحرارية والمغناطيسية، وهي: السعة الحرارية وعامل المغناطيسية وقابليتها للتمغنط. وتبين مدى اعتمادها على المتغيرات الفيزيائية لمعادلة هاملتون.

تظهر مخططات الطور المغناطيسي لمادة النقطة الكمية كدالة في وجود درجة الحرارة وتأثير رشبا والمجال المغناطيسي.

تبين النتائج أن المجال المغناطيسي ودرجة الحرارة وتردد الحصر بالإضافة لتأثير رشبا والعيوب الطوبولوجية، تؤثر بشكل كبير على الخواص الحرارية والمغناطيسية للنقطة الكمية.

أظهرت النتائج المحوسبة أن مادة النقطة الكمية تغير من نوعها المغناطيسي من مادة غير ممغنطة إلى مادة ممغنطة كما هو موضح في رسومات الطور المغناطيسي. علاوة على ذلك، يظهر سلوك السعة الحرارية للمادة الكمية كدالة للمتغيرات الفيزيائية في هاملتون النقطة الكمية.

تم اختبار النتائج التي حصلنا عليها بالمقارنة مع نتائج نظرية منشورة سابقاً.